Univ. Nal. Autón. México, Inst. Geología,
Revista, vol. 6, núm. 2, 1986, p. 222-242.

THE TEMPERATURE AND PRESSURE CONDITIONS OF GRENVILLE-AGE GRANULITE-FACIES METAMORPHISM OF THE OAXACAN COMPLEX, SOUTHERN MEXICO

Claudia I. Mora[1],
John W. Valley[1] *and*
Fernando Ortega-Gutiérrez[2]

ABSTRACT

The temperature, pressure and fluid conditions at the peak of granulite facies metamorphism have been determined for charnockites, marbles and quartzofeldspathic gneisses in the Grenville-age Oaxacan Complex, southern Mexico. Reintegration of coarsely exsolved perthites coexisting with plagioclase yields internally consistent peak temperature estimates averaging 710 ± 50° C at 7 kb. Texturally homogeneous alkali feldspar has reequilibrated at low temperature. Unusual solid solution of albite (Ab_5 to Ab_{56}) and anorthite ($An_{0.3}$ to An_{16}) in alkali feldspar necessitates extension of the Stormer (1975) determinative curves beyond their explicit composition limits. Smooth extrapolations of these curves result in unreasonably high temperature estimates, up to 990° C, for feldspar pairs in which $X_{Ab,Af} > 0.4$ which suggests that such simple extrapolation is unwarranted. The distribution of albite between coexisting feldspars is consistent with the more complex shape of the Brown and Parsons (1981) graphical two feldspar thermometer. The Haselton and others (1983) equation yields the most self-consistent temperature estimates over the entire range of compositions.

Peak metamorphic pressures were estimated from garnet-pyroxene equilibria. The Newton and Perkins (1982) anorthite + enstatite = $pyrope_{.67}$ $grossular_{.33}$ + quartz geobarometer yields P= 7.5 ± 1 kb. The geobarometer anorthite + ferrosilite = $almandine_{.67}$ $grossular_{.33}$ + quartz (Bohlen *et al.*, 1983) yields P= 7.3 ± 1 kb.

The assemblage dolomite + diopside + forsterite + calcite restricts the metamorphic temperature to 764 ± 30° C at P_{CO_2} = 7 kb, calculating from the 5 kb experimental reversal of the buffering reaction 3 dolomite + 1 diopside = 2 forsterite + 4 calcite + $2CO_2$ by Kase and Metz (1980). At 710° C, the temperature estimated by two-feldspar thermometry, this assemblage buffers the local fluid composition in marble to $X_{CO_2} = 0.5 \pm 0.2$.

The estimated pressures and temperatures are consistent with metamorphic conditions indicated by the occurrence of quartz + K-feldspar + garnet + sillimanite ± biotite in the pelitic gneisses and orthopyroxene + plagioclase ± garnet ± clinopyroxene in the mafic gneisses of the terrane.

RESUMEN

Se determinaron la temperatura, presión y actividad de los fluidos durante la culminación del metamorfismo de la facies de granulita para charnockitas, mármoles y gneises cuarzo-feldespáticos del Complejo Oaxaqueño de edad grenvilliana expuesto en el sur de México.

La reintegración de sus pertitas con exsolución fanerítica en coexistencia con plagioclasa permite estimar temperaturas máximas promedio e internamente consistentes de 710 ± 50° C a 7 kb. El feldespato alcalino texturalmente homogéneo se reequilibró a temperaturas bajas.

La solución sólida poco usual de albita (Ab_5 a Ab_{56}) y anortita ($An_{0.3}$ a An_{16}) en feldespato alcalino requiere de la extensión de las curvas determinativas de Stormer (1975), más allá de sus límites explícitos de composición. La extrapolación de estas curvas resulta en estimaciones de temperatura poco razonables, hasta 990° C, para parejas de feldespato en las cuales $X_{Ab,Af} > 0.4$ sugiere que dicha extrapolación simplista no se justifica. La distribución de la albita entre los feldespatos coexistentes es congruente con la curva más compleja correspondiente al geotermómetro gráfico de dos feldespatos de Brown y Parsons (1981). La ecuación de Haselton y colaboradores (1983) proporciona las estimaciones más consistentes de temperatura sobre la variación total de la composición.

Las presiones culminantes del metamorfismo se estimaron a partir de los sistemas de equilibrio granate-piroxena. El geobarómetro de Newton y Perkins (1982) anortita + enstatita = $piropo_{.67}$ $grosularita_{.33}$ + cuarzo proporciona una presión de 7.5 kb ±1 kb. El geobarómetro anortita + ferrosilita = $almandita_{.67}$ $grosularita_{.33}$ + cuarzo (Bohlen *et al.*, 1983) da una presión de 7.3 ± 1 kb.

1 *Department of Geology, Rice University, Houston, Texas 77251, U.S.A., present address: Department of Geology and Geophysics, University of Wisconsin-Madison, Madison, Wisconsin 53706, U.S.A.*

2 *Instituto de Geología, Universidad Nacional Autónoma de México, Ciudad Universitaria, Delegación Coyoacán, 04510 México, D.F.*

El conjunto dolomita + diopsida = forsterita + calcita restringe la temperatura metamórfica a 764 ± 30° C a una presión de CO_2 de 7 kb, calculadas por los datos experimentales a 5 kb de Kase y Metz (1980) para la reacción 3 dolomita + 1 diópsida = 2 forsterita + 4 calcita + $2CO_2$. Si se usa la temperatura estimada del geotermómetro de dos feldespatos de 710° C y 7 kb, el conjunto mineral mantiene la composición local del fluido en los mármoles a $X_{CO_2} = 0.5 \pm 0.2$.

Las presiones y temperaturas estimadas son congruentes con las condiciones metamórficas indicadas por la presencia de cuarzo-K feldespato-granate-sillimanita ± biotita en los gneises pelíticos y de ortopiroxena-plagioclasa ± granate ± clinopiroxena en los gneises máficos del terreno oaxaqueño.

LIST OF ABBREVIATIONS

ΔG_r = Gibbs free energy of reaction
ΔS_r = entropy change of reaction
ΔV_r = volume change of reaction
$\mu_{i,J}$ = chemical potential of i in J
$X_{i,J}$ = mole fraction of i in J
$\alpha_{i,J}$ = activity of i in J
$\gamma_{i,J}$ = activity coefficient of i in J
W_{AB} = Margules parameter for mixing of A and B

INTRODUCTION

Detailed study of phase equilibria, geothermometry and geobarometry is a fundamental step in characterizing the metamorphic history of a terrane and forms a basis for further studies of metamorphic processes such as heat exchange, metasomatism, metamorphic fluid migration, fluid-rock interactions, and melting. Bohlen and Essenne's (1977) study of geothermometry in the Adirondack Mountains, New York and Ferry's (1976) phase equilibria study of the Waterville-Vassalboro area, Maine, are two examples of fundamental investigations which have spawned numerous quantitative studies of metamorphic phenomena (Ferry, 1979, 1980, 1981; Valley and Essene, 1980a, 1980b; Bohlen *et al.*, 1980). Additionally, testing the self-consistency of different temperature-dependent systems better defines the conditions for which those systems are useful.

Little is known about the 10,000 km^2 terrane near Oaxaca, Mexico which has been metamorphosed under granulite facies conditions (Figure 1). Preliminary mapping and petrography (Bloomfield and Ortega-Gutiérrez, 1975; Ortega-Gutiérrez, 1981) identified mineral assemblages characteristic of high-grade regional metamorphism but no quantitative study of mineral equilibria in the complex has previously been attempted. This report summarizes a petrographic and analytical study of the Oaxacan Complex undertaken in order to determine the temperature and pressure of the peak of metamorphism.

In granulite facies metamorphic rocks, originally homogeneous mixed feldspars commonly show evidence of exsolution and post-metamorphic reequilibration. The relationship between feldspar texture and thermometry was discussed by Bohlen and Essene (1977) and has been further documented in this study. Solid solution of albite (Ab_5 to Ab_{56}) and anorthite ($An_{0.3}$ to An_{16}) in the alkali feldspars was up to 30 and 500% more extensive, respectively, than noted in most previous thermometric studies of granulite facies rocks (Stormer and Whitney, 1977; Bohlen and Essene, 1977; Dahl, 1979; Bohlen *et al.*, 1980; Stoddard, 1980; Perkins *et al.*, 1982). Alkali feldspars with Ab_{37} to Ab_{56} and An_{12} to An_{19} are reported in granulite gneisses from the Scourie Complex, Scotland (O'Hara and Yarwood, 1978; Rollinson, 1982). The applicability of the Stormer (1975) feldspar thermometer to systems with such extensive solid solution, which requires extrapolation of the thermometer beyond its explicit limit, is tested in this study by comparison with isobarically univariant calc-silicate assemblages. The graphical thermometer proposed by Brown and Parsons (1981) and a recent formulation by Haselton and others (1983), which accounts for ternary solid solution and nonideal mixing in plagioclase and alkali feldspar, are also tested. Post-metamorphic reequilibration precluded use of Fe-Ti oxide geothermometry/oxybarometry (Buddington and Lindsley, 1964) and calcite-dolomite geothermometry (Goldsmith and Newton, 1969).

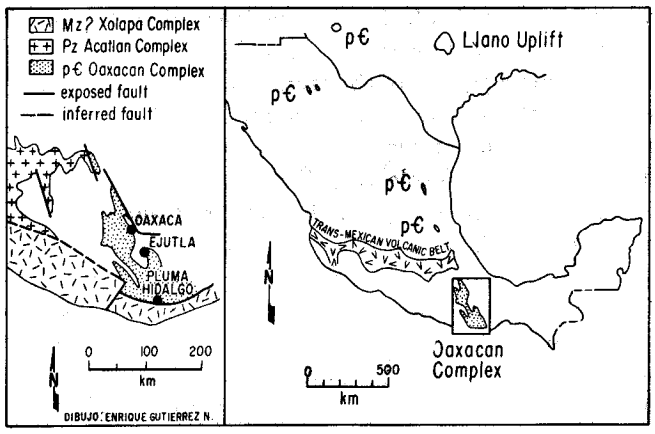

Figure 1.- Location map of the Oaxacan Complex and other exposures of Grenville-age, high-grade metamorphic rock and (inset) younger metamorphic terranes in southern Mexico.

GEOLOGIC SETTING

The Oaxacan Complex is the oldest of several crystalline terranes that crop out in southern Mexico (Figure 1, inset; Ortega-Gutiérrez, 1981). Zircons from

biotite gneiss and syntectonic metamorphic pegmatites in the complex yield nearly concordant U–Pb ages of $1,080 \pm 10$ Ma. Concordant dates of 975 ± 10 Ma for a post-deformational pegmatite give a minimum age for the last significant penetrative deformation (Anderson and Silver, 1971). Fries and others (1966) report Pb-α ages of 240 ± 30 Ma for a post-metamorphic granitic intrusion (Figure 2).

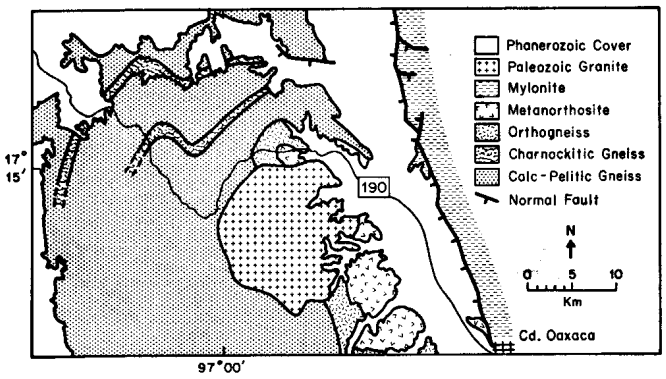

Figure 2.- Generalized geologic map of the northern extent of the Oaxacan Complex, after Ortega-Gutiérrez (1981).

This study was limited to the portion of the complex exposed north of Ejutla (Figure 1, inset). In this area, the complex consists of a basal anorthosite massif (400 km^2), associated mafic orthogneiss, and a diverse upper sequence that includes quartzofeldspathic and biotite-hornblende banded gneisses, charnockites, calc-silicate and pelitic gneisses, and marbles (Figure 2).

The petrography of the area was first summarized by Bloomfield and Ortega-Gutiérrez (1975). Mineral assemblages and sample locations used in the present study are given in Table 1.

The parallel contact of the deformed anorthosite and the overlying gneissic sequence and the absence of a contact metamorphic aureole indicate that intrusion of the anorthosite was premetamorphic. The anorthosite has recrystallized to a coarse, granoblastic texture although relict megacrystic-ophitic texture has been reported (Ortega-Gutiérrez, 1981). Analyses of plagioclase in two samples yield an average composition of An_{47} (Table 2). Common accessory minerals are magnetite, ilmenite, and orthopyroxene. Apatite, quartz, and sphene are less common.

Anorthosite is also reported near Pluma Hidalgo (Paulson, 1964; Heath and Fairbain, 1969; Anderson, 1969), at the extreme southern extent of the complex (Figure 1, inset). Poor exposure and extreme weathering make it difficult to estimate the size of this anorthosite. Accessory minerals are rutile, ilmenite, augite, and apatite. The bulk chemistry is similar to that of the Roseland, Virginia anorthosite (Paulson, 1964). It differs mineralogically from the Oaxacan anorthosite by containing abundant rutile.

Charnockitic gneisses occur in several distinct units in the Oaxacan Complex (Figure 2) and typically contain quartz, K-feldspar, plagioclase, orthopyroxene, clinopyroxene, hornblende, magnetite, and ilmenite. Biotite, apatite, sphene, and zircon are accessory minerals. Interbanded quartzofeldspathic ($\pm$ clinopyroxene $\pm$ magnetite) and biotite-hornblende ($\pm$ garnet $\pm$ K-feldspar $\pm$ plagioclase $\pm$ magnetite $\pm$ ilmenite) gneisses are exposed throughout the complex. Garnet is uncommon and has highly variable composition. Sphene, zircon, apatite, and pyrrhotite are common accessory minerals in both lithologies. The mineralogy of the abundant marbles and calc-silicate gneisses is highly variable and is discussed in greater detail in a later section. Pelitic gneisses (sillimanite-, K-feldspar, cordierite-, or garnet-bearing) have been reported (Bloomfield and Ortega-Gutiérrez, 1975; Ortega-Gutiérrez, 1981) but are not abundant and were not sampled for this study.

Contemporaneously metamorphosed, "Grenville" (1 Ga), high grade metamorphic rocks are exposed in the Oaxacan Complex, the Novillo and Huiznopala Gneisses of northeastern Mexico (Fries and Rincón-Orta, 1965; Ortega-Gutiérrez, 1978), the Sierra del Cuervo, Chihuahua (Mauger and McDowell, 1982), and in the Llano Uplift in central Texas (Garrison, 1979, 1981; Figure 1). The tectonic relationship of these Precambrian exposures is problematic. Correlation of these localities with the Grenville Province of New York and Canada has been proposed because of similarities in their age and lithologies (Fries *et al.*, 1962; Garrison, 1981; Ortega-Gutiérrez, 1981). Interpretations of large-scale displacements across northern Mexico (Silver and Anderson, 1974, 1983), along the Trans-Mexican Volcanic Belt (Gastil and Jensky, 1973), and paleomagnetic evidence for rotation of northern Mexico relative to a stable North America (Urrutia-Fucugauchi, 1981), require greater understanding of the local structure and petrology of these exposures before a coherent tectonic history is possible.

ANALYTICAL PROCEDURE

Quantitative chemical analyses of selected mineral assemblages were made on the ETEC autoprobe at Rice University using an accelerating potential of 15kV and a sample current of 0.015μA. A beam current regulator was used to control drift. Volatilization checks were made for each element by confirming no loss of counts over five consecutive 60 second counting periods. Counting time for wavelength dispersive analysis ranged from 10-30 second per spot, with five-ten spots analyzed on each grain. Well calibrated natural and synthetic crystalline standards were used. Matrix corrections were made using the program EMPADR VII

Table 1.- Mineral assemblages and sample locations. These represent 65 of 167 samples examined. Other sample information is given in Mora (1983).

Sample	*Qtz	Kfs	Pl	Opx	Cpx	Hbl	Bt	Ilm	Mag	Gar	Spn	Ap	Zrn	Other	Latitude	Longitude
Biotite-hornblende-garnet gneisses																
81-OC-31	X	fp	X				X			X*		X		Rt X, Gr H, *$Prp_{55}Alm_{40}Grs_5$	N 16°50'24"	W 96°48'34"
81-OC-55	X	cp	X				X		X	X*			X	Rt X, *$Prp_{55}Alm_{40}Grs_5$	N 17°02'00"	W 96°57'40"
81-OC-109		cp	X		X	X	X		X		X	X	X	Py X	N 17°21'14"	W 97°01'03"
81-OC-116	X	X	X	X			X	X		X			X	Po X, Cal 0	N 17°20'28"	W 96°57'18"
81-OC-122	X	X	X				X			X	X		X		N 17°21'21"	W 96°58'20"
81-OC-124	X	fp	0				X	X	X	X*			X	Chl 0, *$Prp_{20}Alm_{35}Sps_{25}Grs_{20}$	N 17°22'04"	W 96°59'00"
81-OC-143		cp	X			X		X	X		X		X		N 17°22'08"	W 97°02'56"
81-OC-144		cp	X			X	X	X	X		X	X			N 17°22'00"	W 97°03'10"
81-OC-147		X	X				X		X		X				N 17°23'07"	W 97°02'50"
81-OC-161		cp	X			X	X		X		X	X			N 16°56'17"	W 96°59'29"
Orthogneisses																
81-OC-1		X	X	X			X	0	X		X				N 17°07'14"	W 96°53'50"
81-OC-2	X	fp	X	X	X			0	X			X		Hem 0	N 17°07'14"	W 96°53'50"
81-OC-51		X	X	X			X	0	X			X			N 17°01'46"	W 96°55'09"
Anorthosite and nelsonite																
81-OC-9								X	X		X	X			N 17°16'58"	W 96°56'04"
81-OC-11			X					X	X			X		Chl 0	N 17°16'58"	W 96°56'04"
81-OC-13			X	X				X	X			X		Chl 0	N 17°16'58"	W 96°56'04"
81-OC-100	X		X					X				X		Ep 0	N 17°06'35"	W 96°52'10"
81-OC-106	X		X					X				X		Ep 0, Chl 0	N 17°07'19"	W 96°53'18"
81-OC-107A			X					X				X		Clay 0	N 17°07'07"	W 96°49'53"
Charnockite-mangerite gneisses																
81-OC-36	X	cp	X	X			X		0		X			Hem 0	N 16°50'24"	W 96°48'34"
81-OC-38	X	cp	X	X							X			Hem 0, Py X	N 16°50'24"	W 96°48'34"
81-OC-48	X	cp	X	X		X	X	X	X			X			N 16°32'20"	W 96°42'09"
81-OC-71	X	fp	X	X	X	X		X	X		X	X			N 17°20'04"	W 96°07'17"
81-OC-91		cp	X	X	X	X		0	X	X				Po X	N 16°51'47"	W 96°56'34"
81-OC-133	X	X	X	X	X			X	X		X			Gr H	N 17°19'30"	W 97°07'05"
81-OC-134	X	X	X	X	X	X		X				X	X	Py X	N 17°19'30"	W 97°07'05"
81-OC-135		cp	X	X	X	X		0	X		X		X		N 17°19'00"	W 97°06'40"
81-OC-145	X	cp	X	X	X	X	X	X	X		X				N 17°22'16"	W 97°02'49"
81-OC-160		cp	X	X	X	X						X	X		N 16°56'17"	W 96°59'29"
81-OC-167A		X	X	X	X	X	X					X		Py X, Cal 0	N 16°56'40"	W 96°49'48"
Quartzofeldspathic gneisses																
81-OC-4	X	cp	X												N 17°06'22"	W 96°55'47"
81-OC-5	X	fp	X												N 17°06'07"	W 96°56'36"
81-OC-6	X	cp	X							X					N 17°06'07"	W 96°56'36"
81-OC-37	X	cp	X						X		X			Ep 0, Cal 0, Hem 0	N 16°50'24"	W 96°48'34"
81-OC-56	X	cp	X				X		X				X		N 17°02'00"	W 96°57'40"
81-OC-67	X	fp	X	X	X									Gr X	N 17°19'45"	W 96°95'08"
81-OC-89	X	fp	X		X						X	X		Scp X, Cal 0	N 16°51'47"	W 96°56'34"
81-OC-119	X	cp	X	?				X	X			X			N 17°20'53"	W 96°58'02"
81-OC-149	X	cp	X			X	X		X			X	X	Hem 0	N 17°22'42"	W 97°02'43"
81-OC-149A	X	cp	X			X	X		X			X	X		N 17°22'42"	W 97°02'43"
81-OC-150	X	X	X		X			X						Gr H	N 17°17'02"	W 97°07'28"
81-OC-152	X	fp	X					X	X						N 17°17'48"	W 97°08'56"
81-OC-158	X	cp	X												N 16°56'17"	W 96°59'37"

(Rucklidge and Gasparrini, 1969). The accuracy of reported analyses is ±3% of the amount present for major elements and ±5–10% of the amount present for elements with < 1 weight percent abundance.

Feldspars were analyzed for Na, K, Ca, Ba, Al, and Si. Perthitic feldspar was reintegrated by averaging analyses of 50–150 spots on each perthite grain, after the method of Bohlen and Essene (1977). A slightly defocused 20μ beam was used. Plagioclases were homogeneous and five spots were analyzed on each grain. Feldspar pairs 81-OC-71 and 81-OC-145 were analyzed for Fe (Table 3) yielding 0.09–0.14 weight percent Fe_2O_3, but Fe was generally not detected in the feldspar by energy dispersive analyses.

Analyses presented in Tables 4 and 5 represent average analyses of three to four grains per thin section. There was no chemical zonation in garnet, pyroxene, plagioclase, or forsterite and, on the scale of a thin section, the major elements in each phase varied by $\leq$ 2% of the amount present.

ANALYTICAL RESULTS AND DISCUSSION

FELDSPAR EXSOLUTION TEXTURES

In granulite facies metamorphic rocks, originally homogeneous mixed feldspars commonly show evidence of exsolution and post-metamorphic reequilibration. Exsolution textures vary considerably, depending partly on the post-metamorphic thermal and strain histories of the rock, the presence of intergranular fluids, and the relative proportions of the host and included phases. Perthite is common in feldspars from banded gneisses and charnockites in the Oaxacan Complex.

Perthite exsolution textures observed in Oaxacan

Table 1.- Mineral assemblages and sample locations. These represent 65 of 167 samples examined. Other sample information is given in Mora (1983) (*continuation*).

Sample	Cal	Dol	Cpx	Fo	Phl	Wo	Qtz	Kfs	Pl	Scp	Srp	Gr	Other	Latitude	Longitude
Marbles and calc-silicate gneisses															
81-OC-22	X		X					X	X	X			Spn X	N 17°17'07"	W 96°59'30"
81-OC-24			X							X			Spn X	N 17°17'07"	W 96°59'30"
81-OC-25	X		X				X	X		X		X	Spn X, Po X	N 17°17'07"	W 96°59'30"
81-OC-27	X		X				X	fp		X			Spn X, Ap X, Po X	N 17°15'16"	W 96°00'18"
81-OC-28	X		X			X	X	X	X				Spn X, Zo 0, Ap X	N 16°50'24"	W 96°48'34"
81-OC-29	X					X	X							N 16°50'24"	W 96°48'34"
81-OC-30	X					X	X		X					N 16°50'24"	W 96°48'34"
81-OC-32	XO		X			X	X	cp						N 16°50'24"	W 96°48'34"
81-OC-34	X		X			X	X	fp	X	X				N 16°50'24"	W 96°48'34"
81-OC-35	X		X	X					X					N 16°50'24"	W 96°48'34"
81-OC-40	X	0	X	X	X									N 16°45'09"	W 96°51'31"
81-OC-42	X										0	H		N 16°51'35"	W 96°44'10"
81-OC-81	X		X				X		X	X				N 17°15'40"	W 96°59'46"
81-OC-82B	X		X				X	cp	X	X			Spn X	N 17°13'50"	W 97°00'26"
81-OC-85	X	X	X	X	X					X	0		Po X	N 16°51'12"	W 96°55'25"
81-OC-93	X	X		X							0	H		N 16°47'22"	W 96°51'30"
81-OC-94	X	X	X	X	X					X			Ap X	N 16°47'35"	W 96°51'14"
81-OC-95	X	XO	X	X	X						0	H		N 16°47'48"	W 96°51'13"
81-OC-96	X	XO	X	X	X							H	Po X	N 16°47'50"	W 96°50'59"
81-OC-99	X					X	X	cp		0			Sp X	N 16°47'42"	W 96°51'25"
81-OC-113	X	0	X		X			X		X		H	Ap X	N 17°10'10"	W 96°00'34"
81-OC-121	X		X				X					X	Ap X	N 17°21'20"	W 96°58'13"
81-OC-136	X		X				X	cp		X	X	H	Spn X, Po X, Zo 0	N 17°18'22"	W 97°05'05"

* Mineral abbreviations: Alm=Almandine, Ap=Apatite, Bt=Biotite, Cal=calcite, Chl=chlorite, cp=coarsely-exsolved perthite, Cpx=clinopyroxene, Dol=dolomite, Ep=epidote, Fo=forsterite, fp=finely-exsolved perthite, Gar=garnet, Gr=graphite, Grs=grossular, Hbl=hornblende, Hem=hematite, Ilm=ilmenite, Kfs=K-feldspar, Mag=magnetite, Opx=orthopyroxene, Phl=phlogopite, Pl=plagioclase, Po=pyrrhotite, Prp=pyrope, Py=pyrite, Otz=quartz, Rt=rutile, Scp=scapolite, Spn=sphene, Sps=Spessartine, Srp=serpentine, Wo=wollastonite, Zo=zoisite, Zrn=zircon

**Symbols used: X = primary phase, 0 = secondary phase, H = phase seen in hand specimen only.

Table 2.- Plagioclase analyses from the Oaxacan anorthosite massif.

	81-OC-107A			81-OC-100		
	PL-1	PL-2	PL-3	PL-1	PL-2	PL-3
SiO_2	63.04	62.41	62.34	60.89	60.86	62.14
TiO_2	<0.05	<0.05	<0.05	<0.05	0.05	<0.05
Al_2O_3	24.72	24.39	24.54	24.60	24.53	24.38
Fe_2O_3	0.10	0.22	0.13	0.19	0.17	0.14
MnO	0.05	<0.05	<0.05	<0.05	<0.05	0.13
MgO	<0.05	<0.05	0.06	<0.05	0.08	<0.05
CaO	6.62	6.48	6.69	6.10	6.21	6.33
Na_2O	6.84	6.86	6.53	7.39	7.29	7.05
K_2O	0.26	0.38	0.32	0.15	0.23	0.18
Total	101.63	100.74	100.61	99.32	99.42	100.35
Formulae normalized to 5 cations						
Si	2.797	2.790	2.794	2.758	2.753	2.788
Al	1.242	1.235	1.246	1.262	1.257	1.239
Mn	0.004	0.000	0.000	0.000	0.000	0.010
Mg	0.000	0.000	0.003	0.000	0.005	0.000
Fe^{3+}	0.007	0.015	0.009	0.013	0.011	0.010
Na	0.482	0.487	0.464	0.531	0.523	0.502
Ca	0.449	0.443	0.458	0.422	0.430	0.434
K	0.020	0.030	0.025	0.012	0.018	0.014
O	8.172	8.157	8.176	8.122	8.120	8.152
%An	47.3	46.7	48.4	43.7	44.3	45.7
%Ab	50.6	50.7	49.0	55.0	53.8	52.8
%Or	2.1	3.1	2.6	1.3	1.9	1.5

[1] Calculated from normalized formula.

samples are shown in Figure 3. A spectrum of textures, from homogeneous to very coarsely exsolved, is noted.

Figure 3a shows a coexisting pair of homogeneous plagioclase and alkali feldspar. Triple point grain intersections (120°) suggest that the minerals represent metamorphic equilibrium (Spry, 1969). However, feldspar pairs with this texture yield unreasonably low metamorphic temperatures of < 500° C at 7 kb using the Haselton and others (1983) geothermometer (Table 2). Much of the albite component in these alkali feldspars has apparently exsolved and completely diffused to the grain boundary during post-metamorphic reequilibration.

Microcline twinning is sometimes seen, as in Figure 3b, and is indicative of retrograde $(Al\text{-}Si)^{IV}$ ordering at low temperature. It is shown in the same thin section with a bead perthite and plagioclase. Perthite textures are classified after Spry (*op. cit.*). Feldspars with textures intermediate between alkali feldspars, in which the exsolved albite has completely diffused to the grain boundary, and coarsely exsolved perthites are typically rod perthites such as seen in Figure 3c. Coarse ribbon textures are shown in Figures 3d-g. Mesoperthite textures, such as that seen in Figure 3h, are not classified by Spry (1969) and are here designated "convoluted". Coarse ribbon and convoluted textures are also noted in granulite facies gneisses from the Scourie Complex, Scotland (Rollinson, 1982).

Reintegrated microprobe analysis and estimated temperatures for coexisting feldspar are included in Table 3. If exsolution is strictly intragranular, then reinte-

Table 3.- Coexisting plagioclase and alkali-feldspar.

	81-OC-1		81-OC-4*		81-OC-5p		81-OC-6*		81-OC-36*	
	kfs	plag	kfs	plag	kfs	plag	kfs	plag	kfs	plag
SiO_2	63.11	60.72	64.21	63.98	64.76	62.17	63.52	61.80	65.02	64.82
Al_2O_3	19.21	25.48	21.59	23.66	18.99	24.18	20.72	23.97	19.29	22.04
BaO	2.21	<0.05	0.65	0.51	0.19	<0.05	<0.05	<0.05	0.64	0.52
CaO	0.08	6.84	2.25	4.47	0.25	5.50	2.18	5.47	0.85	2.70
Na_2O	0.71	6.65	5.62	8.57	1.71	9.06	3.75	7.56	5.15	9.03
K_2O	14.85	0.31	6.58	0.25	14.41	0.18	9.11	0.17	9.22	0.37
Total	100.17	100.00	100.90	101.44	100.31	101.99	99.28	98.97	100.17	99.48
Formulae normalized to 5 cations										
Si	2.948	2.726	2.876	2.811	2.965	2.718	2.908	2.789	2.938	2.897
Al	1.058	1.348	1.140	1.226	1.025	1.246	1.118	1.275	1.027	1.161
Na	0.064	0.579	0.488	0.730	0.152	0.768	0.333	0.661	0.451	0.782
Ca	0.004	0.329	0.108	0.210	0.012	0.258	0.107	0.265	0.041	0.129
K	0.885	0.018	0.376	0.014	0.842	0.010	0.532	0.010	0.531	0.021
Ba	0.040	0.000	0.011	0.009	0.000	0.000	0.000	0.000	0.011	0.009
O	8.001	8.102	8.013	8.052	7.986	7.952	8.033	8.091	7.960	8.075
%An	0.4	35.5	11.1	22.0	1.2	24.9	11.0	28.3	4.0	13.8
%Ab	6.7	62.6	50.2	76.5	15.1	74.1	34.3	70.6	44.1	83.9
%Or	92.9	1.9	38.7	1.5	83.7	1.0	54.7	1.1	51.9	2.3
T1	470		900		570		805		760	
T2	495		815		585		790		725	
T3	450		730		575		700		720	

	81-OC-37		81-OC-38		81-OC-48*		81-OC-55		81-OC-56	
	kfs	plag	kfs	plag	kfs	plag	kfs	plag	kfs	plag
SiO_2	65.55	64.68	64.24	63.44	65.57	62.81	64.06	62.27	64.52	63.01
Al_2O_3	19.99	23.22	20.96	22.92	21.69	23.56	21.60	24.59	20.09	23.68
BaO	0.71	0.61	0.53	0.55	0.18	<0.05	0.66	0.46	0.88	0.58
CaO	0.90	3.90	2.31	4.15	2.78	4.65	2.54	5.66	1.04	4.55
Na_2O	4.62	8.73	5.76	8.25	5.99	8.22	4.23	7.84	3.06	8.43
K_2O	10.16	0.27	5.90	0.22	4.80	0.15	8.58	0.24	11.85	0.27
Total	101.93	101.41	99.70	99.53	101.01	99.39	101.67	101.06	101.44	100.52
Formulae normalized to 5 cations										
Si	2.919	2.843	2.911	2.848	2.929	2.811	2.869	2.755	2.917	1.795
Al	1.049	1.203	1.120	1.213	1.142	1.243	1.141	1.282	1.068	1.238
Na	0.399	0.744	0.506	0.718	0.519	0.713	0.367	0.673	0.267	0.725
Ca	0.043	0.184	0.112	0.200	0.133	0.223	0.122	0.268	0.050	0.216
K	0.577	0.015	0.341	0.012	0.273	0.008	0.490	0.014	0.682	0.015
Ba	0.012	0.011	0.009	0.010	0.003	0.000	0.012	0.008	0.016	0.010
O	7.955	8.065	8.047	8.091	8.103	8.070	8.012	8.053	7.977	8.043
%An	4.2	19.5	11.7	21.5	14.4	23.6	12.4	28.1	5.0	22.6
%Ab	39.2	78.9	52.7	77.2	56.1	75.6	37.5	70.5	26.7	75.8
%Or	56.6	1.6	35.6	1.3	29.5	0.8	50.1	1.4	68.3	1.6
T1	770		910		990		840		690	
T2	760		805		805		845		670	
T3	770		705		700		705		665	

Table 3.- Coexisting plagioclase and alkali-feldspar (*continuation*).

	81-OC-71		81-OC-82b		81-OC-91		81-OC-109		81-OC-119*	
	kfs	plag	kfs	plag	kfs	plag	kfs	plag	kfs	plag
SiO_2	62.91	62.89	63.97	65.12	63.99	63.12	65.08	63.12	62.98	62.21
Al_2O_3	18.67	22.73	19.81	22.01	20.73	22.93	20.16	22.80	20.74	23.13
BaO	0.94	0.16	0.34	<0.05	0.29	<0.05	0.49	0.43	0.43	0.20
CaO	0.13	4.74	1.51	5.38	3.06	5.20	1.53	4.02	2.64	5.08
Na_2O	1.37	7.84	2.66	7.12	4.75	7.52	5.06	8.33	4.43	7.68
K_2O	14.91	0.19	12.23	0.14	6.54	0.14	8.38	0.31	7.60	0.19
Total	98.93	98.55	100.52	99.77	99.37	98.91	100.70	99.01	98.81	98.49
Formulae normalized to 5 cations										
Si	2.936	2.851	2.912	2.964	2.925	2.856	2.927	2.845	2.897	2.824
Al	1.027	1.215	1.063	1.135	1.117	1.223	1.069	1.211	1.125	1.238
Na	0.124	0.689	0.235	0.514	0.421	0.660	0.441	0.727	0.395	0.678
Ca	0.007	0.230	0.074	0.374	0.150	0.252	0.074	0.194	0.130	0.247
K	0.888	0.011	0.710	0.011	0.382	0.008	0.481	0.018	0.446	0.011
Ba	0.017	0.003	0.006	0.000	0.005	0.000	0.009	0.008	0.008	0.004
O	7.946	8.111	7.971	8.267	8.082	8.133	8.002	8.081	8.040	8.101
%An	0.7	24.7	7.3	29.2	15.7	27.4	7.4	20.7	13.4	26.4
%Ab	12.2	74.1	23.1	69.9	44.2	71.7	44.3	77.4	40.6	72.4
%Or	87.1	1.2	69.6	0.9	40.1	0.9	48.3	1.9	46.0	1.2
T1	535		685		905		830		855	
T2	530		675		855		795		820	
T3	530		635		660		760		675	

	81-OC-124		81-OC-134*		81-OC-135*		81-OC-136*		81-OC-143*	
	kfs	plag	kfs	plag	kfs	plag	kfs	plag	kfs	plag
SiO_2	63.83	64.12	64.08	57.43	67.72	67.39	65.38	65.00	65.40	64.61
Al_2O_3	19.50	21.64	18.26	26.92	19.73	21.85	20.63	22.15	18.96	22.00
BaO	0.44	0.49	0.55	<0.05	<0.05	<0.05	0.13	<0.05	<0.05	<0.05
CaO	0.88	2.19	0.17	9.24	0.73	2.57	1.63	4.52	0.84	3.48
Na_2O	3.66	9.24	0.54	5.55	5.82	9.22	4.34	8.20	4.33	8.70
K_2O	10.74	0.34	15.53	0.26	7.17	0.12	8.96	0.18	9.61	0.14
Total	99.04	98.03	99.13	99.40	101.17	101.15	101.07	100.05	99.26	98.93
Formulae normalized to 5 cations										
Si	2.936	2.900	2.998	2.606	3.018	2.957	2.936	2.899	2.990	2.902
Al	1.057	1.154	1.008	1.441	1.036	1.131	1.092	1.164	1.022	1.165
Na	0.326	0.811	0.049	0.489	0.503	0.785	0.378	0.709	0.384	0.757
Ca	0.043	0.106	0.003	0.449	0.035	0.121	0.078	0.216	0.041	0.167
K	0.630	0.020	0.927	0.015	0.408	0.006	0.513	0.010	0.561	0.008
Ba	0.006	0.009	0.010	0.000	0.000	0.000	0.003	0.000	0.000	0.000
O	7.985	8.062	8.009	8.075	8.081	8.127	8.037	8.120	8.027	8.101
%An	4.3	11.2	0.3	47.1	3.7	13.3	8.1	23.1	4.2	17.9
%Ab	32.4	85.7	5.0	51.3	53.2	86.0	39.0	75.8	38.9	81.2
%Or	62.6	2.1	94.7	1.6	43.1	0.7	52.9	1.1	56.9	0.9
T1	675		465		775		800		750	
T2	670		485		690		775		730	
T3	615		415		730		730		730	

Table 3.- Coexisting plagioclase and alkali-feldspar (*continuation*).

	81-OC-144*		81-OC-145		81-OC-147		81-OC-149*		81-OC-149A*	
	kfs	plag	kfs	plag	kfs	plag	kfs	plag	kfs	plag
SiO_2	65.06	64.47	65.85	63.62	67.41	64.81	65.44	64.16	65.34	64.75
Al_2O_3	20.40	22.20	18.82	24.28	19.58	23.37	19.86	22.45	19.67	22.05
BaO	1.06	0.54	0.16	<0.05	0.60	0.50	0.40	0.36	0.22	0.15
CaO	1.29	3.49	0.47	6.11	0.46	4.50	1.03	3.38	1.34	3.58
Na_2O	5.48	8.72	2.31	7.11	5.42	8.38	4.26	9.26	4.49	8.69
K_2O	7.45	0.24	12.85	0.17	8.51	0.25	10.07	0.27	8.92	0.16
Total	100.47	99.66	101.46	100.99	101.98	101.81	101.06	99.88	99.98	99.38
Formulae normalized to 5 cations										
Si	2.930	2.883	3.024	2.814	2.994	2.844	2.942	2.847	2.966	2.898
Al	1.083	1.170	1.004	1.272	1.025	1.209	1.052	1.174	1.053	1.164
Na	0.478	0.756	0.203	0.613	0.467	0.713	0.371	0.797	0395	0754
Ca	0.062	0.167	0.023	0.291	0.022	0.212	0.050	0.161	0065	0172
K	0.428	0.014	0.742	0.010	0.482	0.014	0.578	0.015	0517	0009
Ba	0.019	0.009	0.003	0.000	0.010	0.009	0.007	0.006	0004	0003
O	8.019	8.082	8.056	8.140	8.032	8.086	7.949	8.028	8.037	8.103
%An	6.4	17.8	2.4	31.8	2.3	22.6	5.0	16.5	6.7	18.4
%Ab	49.4	80.7	21.0	67.1	48.1	75.9	37.1	82.0	40.4	80.6
%Or	44.2	1.5	76.6	1.1	49.6	1.5	57.9	1.5	52.9	1.0
T1	825		675		885		730		765	
T2	760		675		830		715		745	
T3	755		710		990		690		695	

	81-OC-152*		81-OC-158*		81-OC-160	
	kfs	plag	kfs	plag	kfs	plag
SiO_2	63.92	62.32	65.01	63.58	63.57	62.39
Al_2O_3	19.74	22.66	20.29	22.96	22.13	23.59
BaO	0.57	0.57	0.90	0.57	0.52	0.21
CaO	1.27	4.39	1.05	3.27	2.32	4.67
Na_2O	4.01	10.39	4.15	8.96	5.67	8.18
K_2O	9.68	0.20	10.36	0.30	5.53	0.29
Total	99.19	100.53	101.76	99.64	99.74	99.33
Formulae normalized to 5 cations						
Si	2.935	2.725	2.911	2.835	2.879	2.797
Al	1.068	1.168	1.071	1.207	1.181	1.247
Na	0.357	0.881	0.360	0.775	0.498	0.711
Ca	0.062	0.206	0.050	0.156	0.113	0.224
K	0.567	0.011	0.592	0.017	0.319	0.016
Ba	0.010	0.010	0.016	0.010	0.009	0.003
O	8.006	7.864	7.971	8.043	8.060	8.055
%An	6.3	18.8	5.0	16.5	12.1	23.6
%Ab	36.2	80.2	35.9	81.7	53.6	74.7
%Or	57.5	1.0	59.1	1.8	34.3	1.7
T1	740		725		975	
T2	720		720		835	
T3	680		685		795	

*Average analysis for 2-4 grains in the same thin section.
T1 calculated using Stormer (1975) thermometer for P = 7 kb.
T2 determined using Brown and Parsons (1981) graphical thermometer as shown in Figure 6.
T3 calculated using (Haselton et al.,1983) thermometer for P = 7 kb.

Table 4.- Mineral analyses for geobarometry.

	81-OC-116 GAR	25277 GAR	81-OC-116 OPX	25277 OPX		81-OC-116 PLAG	25277 PLAG
SiO_2	38.40	37.87	50.67	52.02	SiO_2	63.13	47.21
TiO_2	0.04	0.03	0.08	0.09	Al_2O_3	23.72	33.68
Al_2O_3	22.55	21.70	2.36	1.49	Fe_2O_3	0.26	0.25
Fe_2O_3[1]	0.00	1.30	1.46	0.00	CaO	4.81	16.29
FeO	29.91	25.51	28.86	27.55	Na_2	7.94	1.94
MnO	1.36	0.83	0.40	0.29	K_2O	0.18	0.09
MgO	5.70	5.76	17.38	18.05			
CaO	2.49	6.76	0.21	0.76	Total	100.04	99.46
Total	100.45	99.76	101.42	100.25			
Formulae normalized to 8 cations (gar), 4 cations (pyx), or 5 cations (plag)							
Si	3.001	2.961	1.926	1.985	Si	2.817	2.176
Al^{IV}	0.000	0.039	0.074	0.015	Al	1.248	1.831
Al^{VI}	2.078	1.962	0.032	0.052	Fe^{3+}	0.008	0.009
Ti	0.002	0.002	0.002	0.003	Na	0.687	0.173
Fe^{3+2}	0.000	0.073	0.038	0.000	Ca	0.230	0.805
Mg	0.664	0.671	0.985	1.026	K	0.010	0.005
Fe^{2+}	1.955	1.671	0.921	0.879	O	8.097	8.006
Mn	0.090	0.055	0.013	0.009			
Ca	0.209	0.566	0.008	0.031			
O	12.041	12.000	6.000	6.022			

[1]Calculated from normalized formula.
[2]Fe^{3+} calculated from charge balance assuming no site vacancies.

Table 5.- Clinopyroxene and forsterite analyses.

	81-OC-85 CPX	81-OC-94 CPX	81-OC-95 CPX	81-OC-96 CPX		81-OC-85 FO	81-OC-94 FO	81-OC-95 FO	81-OC-96 FO
SiO_2	53.19	54.76	53.39	54.45	SiO_2	41.76	41.19	40.56	40.88
TiO_2	0.23	0.15	0.26	0.14	FeO	4.23	4.17	5.58	5.47
Al_2O_3	2.56	0.65	1.92	1.04	MnO	0.42	0.61	0.50	0.44
Fe_2O_3[1]	1.05	0.52	1.04	1.02	NiO	0.28	<0.05	<0.05	<0.05
FeO	<0.05	0.30	<0.05	<0.05	MgO	54.07	53.27	52.92	52.23
MgO	18.11	18.50	18.49	18.81	CaO	0.10	<0.05	<0.05	<0.05
CaO	25.06	25.32	25.24	24.94					
Na_2O	0.19	<0.05	<0.05	<0.05	Total	100.86	99.24	99.56	99.02
Total	100.39	100.20	100.34	100.40					
Formulae normalized to 4 cations					Formulae normalized to 3 cations				
Si	1.910	1.974	1.920	1.957	Si	0.990	0.992	0.977	0.992
Al^{IV}	0.090	0.026	0.080	0.043	Mg	1.910	1.912	1.900	1.888
Al^{VI}	0.018	0.002	0.001	0.001	Fe^{2+}	0.084	0.084	0.113	0.111
Ti	0.006	0.004	0.007	0.004	Mn	0.008	0.012	0.010	0.009
Fe^{3+2}	0.028	0.014	0.028	0.028	Ni	0.005	0.000	0.000	0.000
Mg	0.969	0.994	0.991	1.007	Ca	0.003	0.000	0.000	0.000
Fe^{2+}	0.000	0.009	0.000	0.000	O	3.990	3.992	3.977	3.992
Ca	0.964	0.978	0.973	0.960					
Na	0.013	0.000	0.000	0.000					
O	5.976	6.000	5.982	5.997					

[1]Calculated from normalized formula.
[2]Fe^{3+} calculated by charge balance assuming no site vacancies.

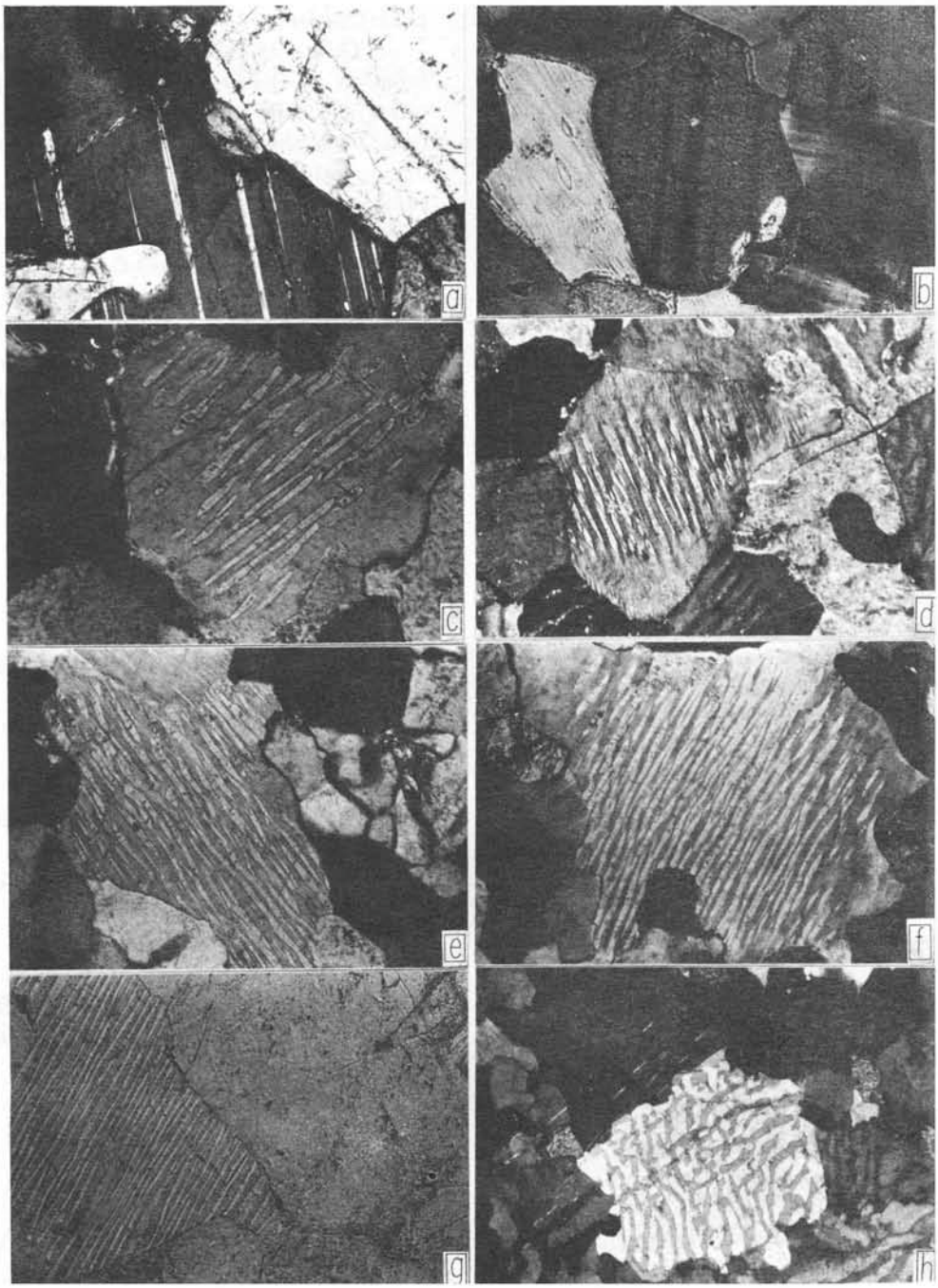

Figure 3.- Photomicrographs of typical perthitic exsolution textures in alkali-feldspars from the Oaxacan Complex. (a) 81–OC–1, texturally homogeneous alkali-feldspar with 120° grain boundary intersections: T = 450° C. (b) 81–OC–5p, homogeneous microcline and bead perthite, for the perthite-plagioclase pair: T = 575° C, for the microcline-plagioclase pair: T = 515° C. (c) 81–OC–56, rod perthite considered to be intermediate between coarsely-exsolved perthites and alkali-feldspars which have exsolved and diffused most of the Ab component. (d) 81–OC–37, coarse rod perthite with thin margin of nearly-homogeneous K-feldspar interpreted as having resulted from secondary grain boundary diffusion: T = 770° C. (e) 81–OC–149, coarsely-exsolved ribbon perthite: T = 690° C. (f) 81–OC–149A, coarsely-exsolved ribbon perthite from thin section cut perpendicular to (e): T = 695° C. (g) 81–OC–38, coarsely-exsolved ribbon perthite, plane polarized light; there are no textural differences between this calcic (An_{12}) alkali-feldspar and a less calcic (81–OC–37, An_4) sample: extrapolation of the Stormer (1975) curves using his thermometric equation yields T = 912° C, the temperature calculated using Haselton and coworkers' (1983) is 705° C. (h) 81–OC–117, "convoluted" texture of a mesoperthite from a one-feldspar rock: no temperature is estimated. Classification of the textures is after Spry (1969). Temperatures are estimated using the Haselton and coworkers' (1983) two-feldspar thermometer. Field of view: (a) and (b) 846 × 570μm; (c), (d), (e), and (f) 1320 × 870μm; (g) 1050 × 705μm; (h) 4050 × 2700μm.

gration of the exsolved phase into the host should yield peak metamorphic compositions and hence, peak temperature. It is possible, however, that there has been loss of Na or K due to secondary grain boundary diffusion over the long cooling history of the rock. Therefore, the reintegrated analyses yield minimum estimates of temperatures for peak metamorphic conditions.

There is a striking corresponce between the estimated temperatures and the extent of exsolution in the alkali feldspars. This relationship was first documented in granulite facies gneisses from the Adirondacks by Bohlen and Essene (1977). Feldspar pairs showing no perthitic exsolution, such as in sample 81–OC–1 (Figure 3a and Table 2), yield temperatures < 500° C at 7 kb (Stormer, 1975). In sample 81–OC–5 (Figure 3b), the microcline-plagioclase pair yields $T = 515°$ C while the bead perthite-plagioclase pair gives $T = 575°$ C. Coarsely exsolved ribbon perthites, such as 81–OC–37 (Figure 3d), yield much higher temperatures of 700 to 800° C. Rod perthites, such as 81–OC–56 (Figure 3c), appear to have lost some of their albite component by exsolution and diffusion and yield temperatures that are intermediate compared to the above extremes. In this case, $T = 665°$ C. In this and previous studies, reintegration of coarse perthites yields internally consistent temperature estimates of 675 to 800° C that are reasonable for granulite facies metamorphism (Winkler, 1979) and have been shown to be consistent with other mineral thermometers (Bohlen and Essene, 1977; Stormer and Whitney, 1977; Dahl, 1979; Bohlen *et al.*, 1980; Perkins *et al.*, 1982) and phase equilibria (Stormer and Whitney, 1977; Valley and Essene, 1980a, 1980b; this study).

This textural interpretation is supported by results of two feldspar thermometry of granulite facies xenoliths (Padovani and Carter, 1978; Matty *et al.*, 1982). Matty and others (*op. cit.*) report high temperatures ($T = 675$ to 700° C) for homogeneous feldspar pairs from crustal xenoliths in lavas from Craters of the Moon National Monument, Idaho. The charnockite xenoliths are interpreted to have been brought rapidly to the surface from the lower crust by the lavas rather than slowly cooled and uplifted as in Oaxaca and other typical high-grade terranes. Unmixing of the feldspars in these xenoliths did not occur due to kinetic barriers imposed by the rapid decrease in pressure and temperature.

Secondary grain boundary diffusion often results in a thin margin of non-perthitic feldspar along the edges of a perthite grain. This texture is seen in 81–OC–37 (Figure 3d). Step-wise microprobe analysis from the perthitic core to the grain edge indicates that diffusion of Na has occurred from the margin of the grain outwards. Discrete, small grains of secondary plagioclase may be formed along the grain boundary. Reintegration of the entire grain would thus underestimate the extent of albite solid solution in the alkali feldspar. Restricting analysis to the perthitic core gives a much better estimate of peak metamorphic composition, and therefore peak temperature, as well.

Thin sections were cut perpendicular to visible foliation in the rocks. If perthite ribbons are crystallographically controlled, but not parallel to foliation, then the extent of perthitic solid solution may be misestimated. To investigate that possibility, mutually perpendicular thin-sections, 81–OC–149 and 81–OC–149A, were cut from a weakly foliated, biotite-quartzofeldspathic gneiss. Optically, there is no difference in the feldspar texture (Figure 3e and f). Three feldspar pairs were analyzed in each thin-section. The average compositions of these feldspars are nearly the same and yield temperatures within the error of the thermometers employed (Table 2). Hence, orientation bias does not appear to be a significant problem or is accounted for by averaging several analyses from each thin-section.

FELDSPAR COMPOSITIONS

Ternary feldspar compositions have been plotted in Figure 4. The wide range of composition reflects the variety of perthite textures analyzed. For coarsely exsolved perthites, the range of compositions is $X_{Ab,Af} = 0.36–0.54$ and $X_{An,Af} = 0.02–0.16$. Plagioclases coexisting with those perthites have variable compositions with $X_{Ab,Pl} = 0.70–0.84$.

Alkali feldspars in the Oaxacan Complex are more albite- and more anorthite-rich than those normally reported from several other granulite facies terranes. Stormer and Whitney (1977) reported $X_{Ab,Af} = 0.20–0.30$ in sapphirine-bearing granulites from Brazil. Alkali feldspars reported from the Adirondack Moun-

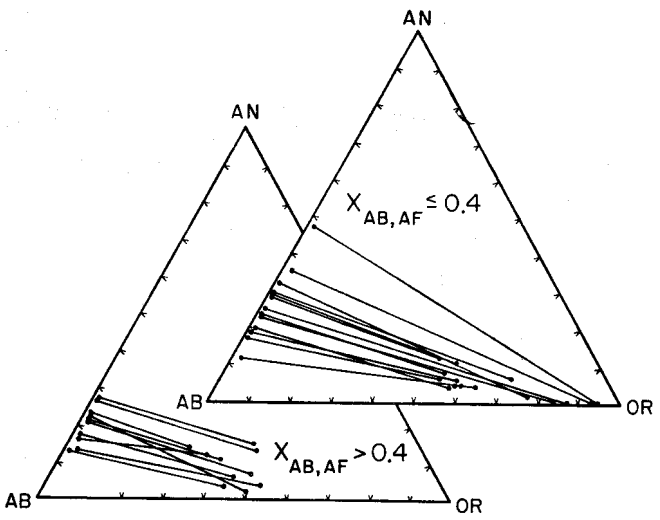

Figure 4.- Ternary compositions of coexisting feldspar pairs from the Oaxacan Complex.

tains, New York, have $X_{Ab,Af}$ = 0.25–0.40 (Bohlen *et al.*, 1980). In both studies, $X_{An,Af} < 0.03$. Charnockite xenoliths from Craters of the Moon, Idaho (Matty *et al.*, 1982) have $X_{Ab,Af}$ = 0.20–0.45 and $X_{An,Af} <$ 0.04. Only in the Scourie Complex, Scotland have compositions of alkali feldspars in granulite gneisses been reported that are similar to the Oaxacan samples with $X_{Ab,Af}$ = 0.37–0.56 and $X_{An,Af}$ = 0.12–0.19 (O'Hara and Yarwood, 1978; Rollinson, 1982). Differences in bulk composition or retrograde diffusion of Ca from alkali feldspar may explain the variability of $X_{An,Af}$ in the different terranes.

With the exception of compositions, reported by O'Hara and Yarwood (1978), $X_{Or,Pl}$ in slowly cooled high grade terranes is < 0.02. Experimental studies on the ternary feldspar system (Seck, 1971; Johannes, 1979) show greater miscibility of K in plagioclase coexisting with alkali feldspars. Values of $X_{Or,Pl}$ are closest to the experimentally determined value in feldspars from granulite xenoliths, whether the feldspars are texturally homogeneous (Matty *et al.*, 1982) or perthitic (Padovani and Carter, 1977). The discrepancy between the experimental and the field data from slowly cooled terranes suggests retrograde diffusion of K from natural plagioclases, rather than poor experimental calibration of the ternary system. The effect of retrograde K diffusion from plagioclase would be to effectively increase $X_{Ab,Pl}$, resulting in a decrease in estimated temperature (Haselton *et al.*, 1983) of up to 50° C.

TWO-FELDSPAR THERMOMETRY

The Stormer (1975) geothermometer is based on the partitioning of albite between plagioclase and alkali feldspar and takes account of the significant pressure dependence of the feldspar system. Stormer (*op. cit.*) adopted a double binary system with ideal solid solution in plagioclase and regular, asymmetric solution in disordered alkali feldspar because lack of ternary activity coefficients precluded thermodynamic modeling of a ternary feldspar system. One of the principal assumptions of this thermometer, then, is that Or has no effect on $\mu_{Ab,Pl}$ and An has no effect on $\mu_{Ab,Af}$ or that the effects cancel. While the validity of this assumption has been questioned (Powell and Powell, 1977; Brown and Parsons, 1981), particularly for An-rich compositions, the thermometer is consistent with existing experimental data on ternary feldspars (Seck, 1971) over a large range of composition and yields consistent temperatures when applied to metamorphic (Bohlen and Essene, 1977; Stormer and Whitney, 1977; Perkins *et al.*, 1982) and igneous rocks (Whitney and Stormer, 1977).

The distribution of albite between coexisting feldspar depends on feldspar structural state as well as pressure and temperature. Whitney and Stormer (*op. cit.*) reformulated Stormer's (1975) thermometer using mixing parameters for ordered alkali feldspars. However, at equilibration temperatures > 665° C, the alkali feldspars are most likely sanidine (Guidotti *et al.*, 1973). Additionally, the Whitney and Stormer thermometer has been shown to be inconsistent with other mineral thermometers in amphibolite facies rock, suggesting that some of the thermodynamic parameters of the thermometer are in error (Nesbitt and Essene, 1982). Thermometers which use mixing parameters for disordered alkali feldspars are thus preferable for granulite facies terranes.

Figure 5 shows coexisting feldspars from the Oaxacan Complex (Table 3) plotted against determinative curves derived from Stormer's mathematical expression. Applicability of these curves is limited to

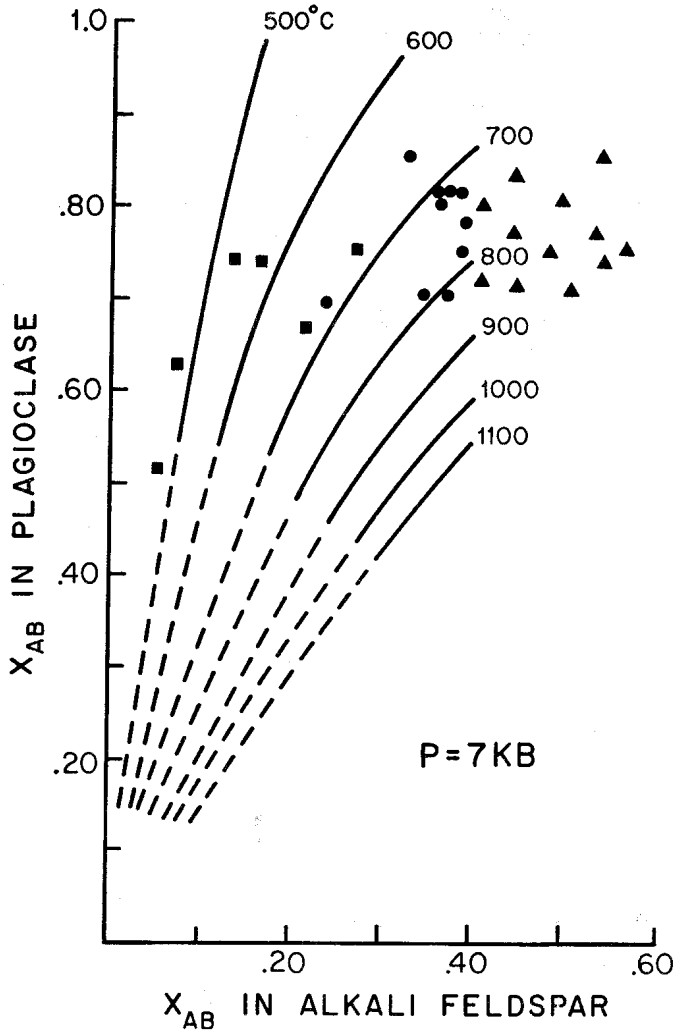

Figure 5.- The distribution of albite between coexisting feldspars as a function of temperature at P= 7 kb, after Stormer (1975). Circles are Oaxacan samples which lie within the specified compositional limits of this thermometer: $X_{Ab,Af} < 0.4$. Triangles are pairs for which $X_{Ab,Af} > 0.4$. Squares are pairs which are interpreted, based on textural criteria, to have reequilibrated at low temperature. An error of ±50° C is estimated.

feldspar compositions for which $X_{Ab,Af} < 0.4$, shown by the area of solid isotherms. The isotherms are dashed as they converge toward $X_{Ab} = 0$ because the activity of albite in plagioclase is not ideal at low $X_{Ab,Af}$ (Orville, 1972; Saxena and Ribbe, 1972). For albite-rich compositions, more ternary solid solution is expected and activity coefficients will differ from the binary coefficients used in formulating the thermometer. Therefore, above $X_{Ab,Af} = 0.4$, Stormer's thermometric equation (Stormer, 1975, p. 670) is not accurate.

The data shown in Figure 5 cluster in the range $0.3 < X_{Ab,Af} < 0.6$. Data shown by circles and triangles represent the compositions of feldspar pairs in which the alkali feldspar is coarsely exsolved rod- or ribbon-perthite. For samples with the composition $0.3 < X_{Ab,Af} < 0.4$, the average temperature is 760 ± 50° C at 7 kb. This estimate includes sample 81-OC-82b, for which $X_{Ab,Af} = 0.23$, because it is texturally more similar to the coarsely exsolved samples than to less coarsely exsolved rod perthites such as 81-OC-56 (Figure 3c), to which it is compositionally similar. Feldspar pairs which plot in the range $X_{Ab,Af} < 0.3$, shown by squares in Figure 5, have homogeneous or less coarsely exsolved perthite textures and are interpreted as having reequilibrated at retrograde conditions based on textural evidence. Hence, these are not included in estimates of peak metamorphic temperature.

Nearly one-half of the Oaxacan samples (shown by triangles in Figure 5) have $X_{Ab,Af} > 0.4$, the limit established by Stormer (*op. cit.*) for application of his thermometer. Extrapolation of Stormer's isotherms beyond their explicit limit yields unreasonably high temperatures (up to 990° C). For example, sample 81-OC-158 ($X_{Ab,Af} = 0.36$) and 81-OC-160 ($X_{Ab,Af} = 0.54$) were collected 800 m apart and have similar mineralogy. No major lithologic changes or structural contacts occur between the two sample locations yet the temperature estimates differ by 250° C. The compositions of coexisting feldspars on 81-OC-158 fall within the limits of Stormer's thermometer and give $T = 725°$ C. The compositions of alkali feldspar in 81-OC-160 fall outside the limits of Stormer's curves. The temperature estimated by Stormer's thermometric equation in this compositional range, $T = 975°$ C, is not consistent with the 725° C estimate for the nearby sample and it exceeds the melting temperature for these rocks, even with relatively low P_{H_2O} (Winkler, 1979).

As a further check on the validity of extrapolating the isotherms to high $X_{Ab,Af}$ using the thermometric equation, one can assume that the regional metamorphic temperatures do not vary greatly across the Oaxacan Complex. The distribution of peak temperature estimates would then lie subparallel to the isotherms (Figure 5). Reasonable error in the temperature estimates widens the range over which the samples plot, but should not significantly alter the geometry of their distribution on the determinative curves. However, the sample distribution is not subparallel to the isotherms but varies over a wide range of $X_{Ab,Af}$ for a relatively restricted range of $X_{Ab,Pl}$ (Figure 5). A contact aureole could explain the 300° C difference suggested by extrapolating the isotherms, but there is no mineralogic or structural evidence to support that hypothesis. Alternatively, more abrupt changes in the slope of the isotherms might be postulated to account for the sample distribution. Isotherms with more horizontal slopes would extend the range over which the mole fraction of albite may vary in an alkali feldspar that maintains isothermal equilibrium with plagioclase of a given composition.

Brown and Parsons (1981) constructed a graphical general form for a two feldspar thermometer based on the ternary experimental data of Seck (1971). This general form is shown in Figure 6. With minor changes, the thermometer is the same as that constructed by Seck (*op. cit.*, fig. 7) for his own data. The shape of the isotherms above $X_{Ab,Af} = 0.4$ reflects the curvature of the isotherms in the ternary system from parallel to the albite-orthoclase join to parallel to the albite-anorthite join. The intersection of the isotherms at the $K_D = 1$ line corresponds with the intersection of the ternary isotherms with the critical solution curve, along which coexisting feldspar pairs come to have the same composition.

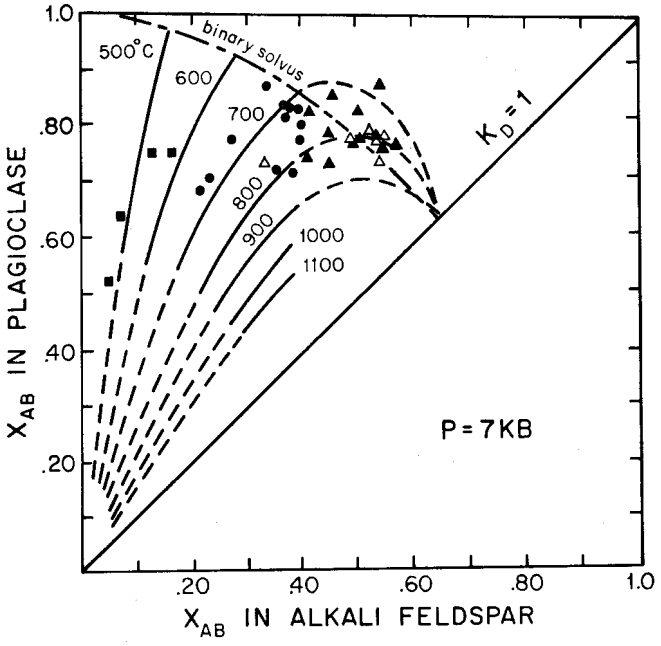

Figure 6.- Coexisting feldspar pairs plotted on the Brown and Parsons (1981) graphical thermometer extrapolated to P= 7 kb. Symbols used are the same as in Figure 5. Open triangles are data from Rollinson (1982) and O'Hara and Yarwood (1978). Solid isotherms are approximately coincident with the Stormer (1975) curves. Isotherms are less accurate in the dashed region and as they converge toward the $K_D = 1$ line.

Below $X_{Ab,Af} = 0.4$, the isotherms for Brown and Parsons' model approximately coincide with Stormer's determinative curves and may therefore be quantitatively correct. Conflicting experimental data on equilibrium ternary feldspar compositions (Johannes, 1979) casts some doubt as to the precision of the constructed isotherms, especially in the compositional range of anorthoclase. Over that range, Brown and Parsons (1981) suggest that the thermometer may be only qualitatively correct. The curvature of the isotherms above $X_{Ab,Af} = 0.4$ extends the range over which the mole fraction of albite may vary in an alkali feldspar in isothermal equilibrium with a plagioclase of a given composition. Hence, if the regional metamorphic temperature does not vary greatly across the Oaxacan Complex then the sample distribution in Figure 6 suggests that the shape and approximate location of the Brown and Parsons (*op. cit.*) isotherms are correct. Temperature estimates using this model are included in Table 2. For feldspars pairs wth $X_{Ab,Af} \leq 0.40$, these estimates are within error of temperatures determined using the Stormer (1975) model. For pairs with more sodic alkali feldspar, the Brown and Parsons (1981) estimates are up to 200° C lower than the Stormer (1975) estimates and are more consistent with the observed mineralogy (Table 1), which indicates metamorphic conditions of the orthopyroxene + plagioclase sub-facies of the granulite facies (De Waard, 1965).

Quantitative use of the Brown and Parsons (1981) thermometer may not be justified due to lack of experimental data on sodic ternary feldspars. However, the temperature estimates using this model are geologically reasonable and consistent, suggesting the graphical thermometer may be quantitatively correct, as well.

The Haselton and coworkers (1983) thermometer combines recent calorimetric data on plagioclase and alkali feldspar and has not yet been applied widely to high grade metamorphic rocks. Because the thermometer accounts for ternary solid solution, use of the graphical form (Haselton *et al.*, *op. cit.*, fig. 8), derived for strictly binary endmembers, requires caution. Isotherms constructed for ternary compositions will shift significantly downward (Mora and Valley, 1985). That difficulty is avoided by using the numerical form of the thermometer:

$$T_k = \Big[(X_{Or,Af})^2(18810 + 17030X_{Ab,Af} + 0.364P_{bars}) - (X_{An,Pl})^2(28230 - 39520X_{Ab,Pl})\Big] \Big/ \left[10.3(X_{Or,Af})^2 + 8.3143 \ln \left\{ \frac{(X_{Ab,Pl})^2(2 - X_{Ab,Pl})}{X_{Ab,Af}} \right\}\right]$$

Temperatures calculated for the Oaxacan samples are given in Table 3 and are consistent for all samples with $X_{Ab,Af} \geq 0.30$. Results for sodic feldspar pairs are up to 300° C lower than the Stormer (1975) estimates and up to 100° C lower than the Brown and Parsons (1981) results.

The results of feldspar thermometry are summarized in Figure 7. The average temperature is 815 ± 85° C (1σ) using Stormer (*op. cit.*), 770 ± 55° (1σ) using Brown and Parsons (*op. cit.*) and 710 ± 40° C ($l\sigma$) using Haselton and coworkers (1983). Both the Brown and Parsons' and Haselton and others' thermometers yield estimates that are consistent, within error, with mineral equilibria in marbles (this study). However, the Haselton and coworkers' results show greater precision and therefore are considered the best estimates of peak metamorphic temperature.

Stormer (1975) assigns an error of ±30° C to his thermometer. The difficulty of reintegrating exsolved perthites contributes to reduced precision, and an error of ±50° C is thus reasonable for temperature estimates using the Stormer's or Haselton and others' model. The error in the Brown and Parsons (1981) thermometer increases as the isotherms converge toward the $K_D = 1$ line.

Temperature estimates for Scourian feldspar pairs with $X_{Ab,Af} > 0.40$ (O'Hara and Yarwood, 1978; Rollinson, 1982) may be similarly made. Extrapolation of Stormer (1975) isotherms yields unreasonably high temperatures of up to 1,100° C at 11 kb. Conditions of granulite-facies metamorphism of the Scourie Complex

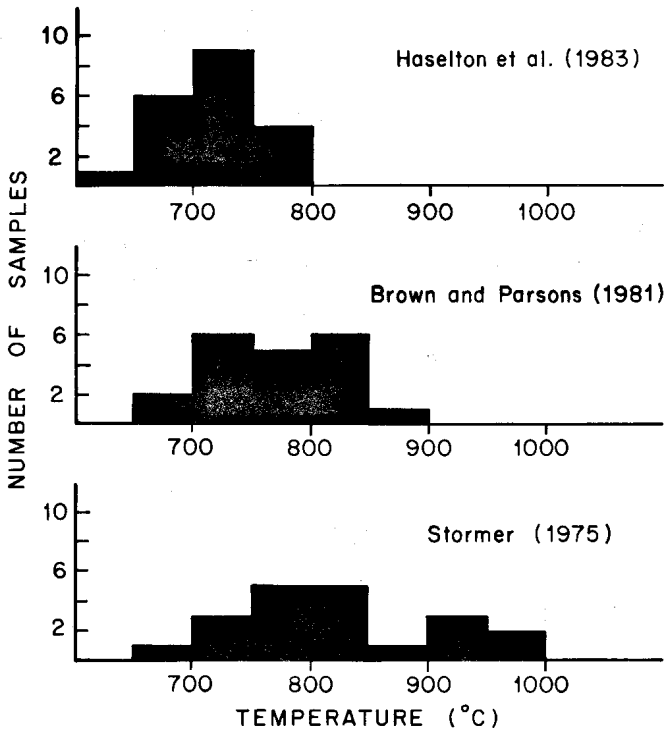

Figure 7.- Summary of feldspar thermometry in the Oaxacan Complex. The results are discussed in the text.

are constrained by garnet-pyroxene (Rollinson, 1981) and magnetite-ilmenite (Rollinson, 1979; 1980) geothermometry to $820 \pm 50°$ C at 11 kb. Plotted against the Brown and Parsons' (1981) isotherms at P= 7 kb (Figure 6), these samples yield a temperature of approximately 800° C. Haselton and coworkers' (1983) thermometer also gives $T = 800°$ C. Hence, for feldspars with those compositions in the Scourie Complex, these two thermometers yield results that are geologically reasonable and more consistent with other temperature dependent systems than results obtained using Stormer's equation.

GARNET-ORTHOPYROXENE BAROMETRY

Two independent calibrations of the barometer plagioclase + orthopyroxene = garnet + quartz:

$$CaAl_2SiO_2O_8 + Mg_2Si_2O_6 = CaMg_2Al_2Si_3O_{12} + SiO_2 \quad (1)$$

anorthite + enstatite
= grossularite$_{.33}$ pyrope$_{.67}$ + quartz

calculated from thermochemical data by Newton and Perkins (1982) and

$$CaAl_2SiO_8 + Fe_2Si_2O_6 = CaFe_2Al_2Si_3O_{12} + SiO_2 \quad (2)$$

anorthite + ferrosilite
= grossularite$_{.33}$ almandine$_{.67}$ + quartz

experimentally located by Bohlen and coworkers (1983), have been used to estimate the metamorphic pressure of the Oaxacan Complex. The reaction is useful as a geobarometer because it has a relatively large ΔV_r and a small ΔS_r [for reaction (2), $\Delta V^\circ_{r,298} = -2.57$ joules/bar and $\Delta S^\circ_{r,298} = -34.55$ joules/mole-° K]. Mineral analyses for this assemblage in two Oaxacan samples are given in Table 4.

Reduced activities due to solid solution in natural mineral assemblages have been calculated using activity models recommended by the respective authors. The standard state is chosen such that the activity (α) of a pure phase is unity at the T, P of interest. The choice of activity model has moderate effect on the calculated pressure.

For reactions (1) and (2), an ideal, two-site ionic solution model was used to calculate the enstatite and ferrosilite activity such that Mg and Fe^{2+} are equipartitioned between the octahedral M1 and M2 sites in orthopyroxene (Wood and Banno, 1973). Thus $\alpha_{En,Opx} = (X_{Mg,M1})(X_{Mg,M2})$ and $\alpha_{Fs,Opx} = (X_{Fe^{2+},M1})(X_{Fe^{2+},M2})$. Using a simple solution model (Saxena, 1973) for orthopyroxene would shift the calculated pressure for reactions (1) and (2) down approximately 0.5 kb for these samples.

Grossularite activities for reactions (1) and (2) have been calculated using a symmetric, three component solution model (Ganguly and Kennedy, 1974):

$$Rt \ln \gamma_{Grs,Gar} = W_{CaFe}X^2_{Fe} + W_{CaMg}X^2_{Mg} + (W_{CaFe} - W_{FeMg} + W_{CaMg})X_{Fe}X_{Mg} \quad (3)$$

Equivalent expressions can be written for the activities of pyrope and almandine. Values for the mixing parameters W_{CaFe}, W_{CaMg} and W_{FeMg} are not well known. Preferred values for reaction (1) are: $W_{CaFe} = 13814 - 6.28T(K)$ J/mol, $W_{CaFe} = 0$ J/mol, and $W_{FeMg} = 0$ J/mol. $W_{FeMg} = 0$ J/mol has been inferred from experimental garnet-olivine exchange (Newton and Haselton, 1981) and natural equilibrium garnet compositions (Hodges and Spear, 1982). For reactions (2), preferred mixing parameters are: $W_{CaMg} = 17497 - 5.02T(°\ C)$ J/mol, $W_{FeMg} = 14567 - 5.02T(°\ C)$ J/mol, and $W_{CaFe} = 4395 - 5.02T(°\ C)$ J/mol. This value of W_{FeMg} is consistent with the value inferred from experimental data on ilmenite-sillimanite-quartz-rutile equilibria (Bohlen *et al.*, 1983). The choice of mixing parameters values can shift calculated pressures by 0.5–1.0 kb.

To calculate anorthite activity, an Al avoidance model is used for reaction (1) (Newton *et al.*, 1980) and experimentally determined activity coefficients (Orville, 1972) for reaction (2). These two approaches yield similar activities over the range $X_{Ab,Pl} < 0.5$. For more calcic compositions the models diverge. The Al-avoidance model predicts $\gamma_{An,PL} < 1$ and the Orville model predicts $\gamma_{An,PL} \approx 1$. Choosing the alternate activity model shifts the calculated pressure by ≤ 0.3 kb for the Oaxacan samples.

Using the designated activity models and mixing parameters, the average calculated metamorphic pressure using reaction (1) is 7.5 kb and for reaction (2) is 7.3 kb (Figure 8). Because of the sensitivity of the barometers to choice of activity models, a reasonable error estimate for these calculations is ± 1 kb. The estimated pressure is consistent (Holdaway, 1971) with the occurrence of sillimanite in the complex.

A barometer based on the solubility of Al in orthopyroxene coexisting with garnet has recently been experimentally calibrated by Harley and Green (1982) in the system CaO-MgO-FeO-Al_2O_3-SiO_2. Application of this new expression was attempted for garnet-orthopyroxene pairs in Table 4. To properly use the barometer, Al must be free to equipartition between the tetrahedral and octahedral Ml sites. However, the presence of Fe^{3+} solid-solution in garnet or orthopyroxene makes nonideal terms important in garnet and may greatly disturb the distribution of Al in Ml. Hence, the barometer appears to be too sensitive to even small

amounts of Fe^{3+} solid-solution and normal analytical inaccuracy affects it to be useful as a quantitative geobarometer.

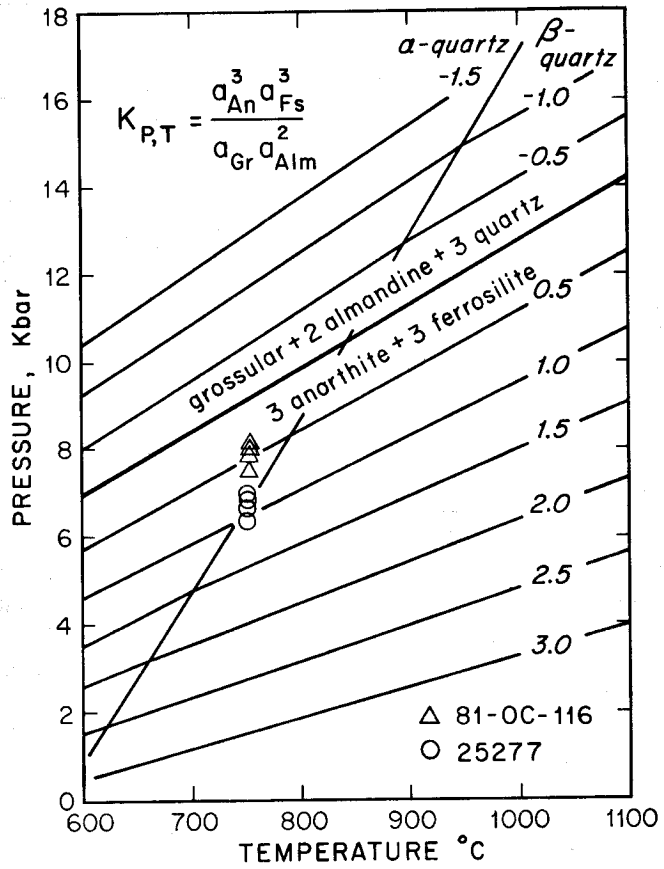

Figure 8.- Schematic $T - X_{CO_2}$ diagram of volatilization reactions in the siliceous dolomite system.

CALC-SILICATE EQUILIBRIA

Abundant marbles and calc-silicate gneisses occur in discontinuous bands and lenses throughout the Oaxacan Complex. Mineral equilibria in the marbles can be used to restrict metamorphic pressure, temperature, and fluid compositions. The stability of reactions in the siliceous dolomite system has been studied experimentally by numerous investigators (Metz, 1967, 1976; Skippen, 1974; Slaughter *et al.*, 1975; Jacobs and Kerrick, 1979, 1981; Eggert and Kerrick, 1981; Kase and Metz, 1980). The isobarically univariant reaction

$$3CaMg(CO_3)_2 + CaMgSi_2O_6 = 4CaCO_3 + 2Mg_2SiO_4 + 2CO_2 \quad (4)$$

3 dolomite + diopside = 4calcite + 2forsterite + $2CO_2$

was studied in four Oaxacan marble samples. Solid solution can extend or restrict the stability of a mineral assemblage and must be evaluated for a quantitative estimate of equilibrium conditions. Microprobe analyses of forsterite and clinopyroxene are given in Table 5.

The location of reaction (4) is disputed (Figure 9). The reaction has been experimentally reversed by Kase and Metz (*op. cit.*) at 1, 3, 5, and 10 kb and by Jacobs (Eggert and Kerrick, 1981) at 4 kb. Additionally, the location of reaction (4) is fixed by the intersection of

$$Tr + 3Cal = Do + 4Di + CO_2 + H_2O \quad (5)$$

with

$$Tr + 11Do = 8Fo + 13Cal + 9CO_2 + H_2O \quad (6)$$

or

$$3Tr + 5Cal = 11Di + 2Fo + 5CO_2 + 3H_2O \quad (7)$$

Location of the invariant point I (Figure 9) from the intersection of reactions (6) and (7) is less accurate as the acute angle of intersection compounds the experimental error.

A compilation of experimental data that restricts the location of reaction (4) for 6 kb is shown in Figure 9. Equilibria has been calculated using the computer program "EQUILI" (Wall and Essene, 1972) which uses an experimentally reversed $P-T-X(\Delta G_r = 0)$ and solves the equation

$$\Delta G_r(P_2T_2XH_2O^2) - \Delta G_r(P_1T_1XH_2O^1) = \int_{T_1}^{T_2} \Delta S_{r(\text{solids})}\,dT + \int_{P_1}^{P_2} \Delta V_{r(\text{solids})}\,dP + \Delta G_{r,\text{fluids}}(P_2T_2XH_2O^2) - \Delta G_{r,\text{fluids}}(P_1T_1XH_2O^1) \quad (8)$$

The sources of thermodynamic data are Robie and others (1979) for S_T and V_{298} solids, Skinner (1966) for thermal expansion, Birch (1966) for compressibility, Burnham and coworkers (1969) for $\Delta G_{f(H_2O)}$, and Wall and Burnham (unpubl. data) for $\Delta G_{f(CO_2)}$.

Using EQUILI, calculation from low pressure reversals to higher pressure yields internally consistent results for the Kase and Metz' (1980) reversals of reaction (4) and the Metz's (1976) reversals of reaction (6). Location of the invariant point I (Figure 9) generated by the intersection of reactions (4), (5), and (6) is approximately 60° C higher than the invariant point I' (Figure 9) generated by Jacobs and Kerrick' (1981) reversal of reaction (4). Location of invariant point I' also restricts the location of reactions (6) and (7) and is incompatible with experimental reversals of reaction (6) (Metz, 1976). At P= 2 kb, reaction (4) is restricted to $X_{CO_2} > 0.8$ by the location of I or I'. However, with increasing pressure, the slope of reactions (4) and (6) becomes more similar, and the range of X_{CO_2} over which reaction (4) is stable is greatly extended. At 6 kb, the uncertainty in the location of I created by the

acute angle intersection of reactions (6) and (7) is nearly $X_{CO_2} = 0.4$. The slope of reaction (5), which is tightly reversed at lower temperatures (Slaughter *et al.*, 1975; Eggert and Kerrick, 1981), becomes more horizontal over this compositional range and does not help to restrict the location of I. Calculations from Kerrick's (unpublished) 2 kb reversal of reaction (7) are inconsistent with both Kase and Metz' and Jacobs and Kerrick' reversals. For 6 kb, the calculations appear to be more consistent, however, with the location of reaction (7) required by the invariant point I than with the location required by invariant point I' (Figure 9).

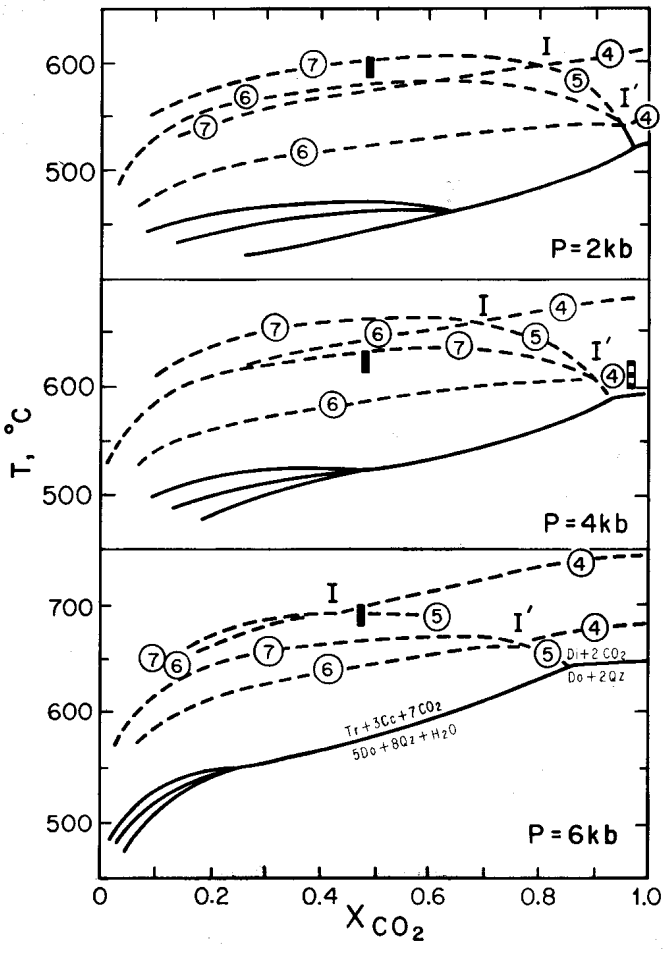

Figure 9.- $T - X_{CO_2}$ diagrams at 2, 4, and 6 kb calculated from experimental brackets for reaction (4) at 1, 3, and 5 kb (Kase and Metz, 1980) and 4 kb by Jacobs (Eggert and Kerrick, 1981), experimental data for reaction (5) at 5 kb (Slaughter *et al.*, 1975) and reaction (6) at 1, 3, and 5 kb (Metz, 1967, 1976). Other reactions are located from experimental brackets at 2, 4, and 6 kb of Eggert and Kerrick (1981). Solid rectangles have been extrapolated from a 2 kb reversal of reaction (7) (Kerrick, personal communication). I and I' are invariant points generated by the location of reaction (4) according to Kase and Metz and Jacobs reversals, respectively.

Uncertainties in experimental and thermochemical data limit the accuracy of calculation of some volatilization reactions from low pressure to higher pressures, as demonstrated by Hunt and Kerrick (1977) for the reaction rutile + calcite + quartz = sphene + CO_2. The largest differences occur when extrapolations are made over a wide range of temperature or X_{CO_2} (Jacobs and Kerrick, 1981). The inconsistency of thermochemical and experimental data may be due in part to nonideality of H_2O-CO_2 mixing and thermodynamic calculations of volatilization reactions using nonideal activities for H_2O and CO_2 calculated from the hard sphere modified Redlich-Kwong equation yields results that are in excellent agreement with the experimental data for many reactions, including reaction (4) (Jacobs and Kerrick, *op. cit.*). Figure 9 demonstrates that multiple reversals at a range of pressures for reactions (4) (Kase and Metz, 1980) and (6) (Metz, 1976) generate a self-consistent phase diagram and are thus consistent with known thermochemical data. In light of the internal consistency and consistency with other experiments and thermodynamic extrapolations from low pressures, the experimental data of Kase and Metz (1980) have been used for equilibria calculations for reaction (4).

At constant pressure and temperature, the shift in reaction equilibria due to solid solution is calculated by the equation

$$\Delta G_r(PTXH_2O^2) - \Delta G_r(PTXH_2O^1) = RT \ln K_{\text{solids}}$$

The activities of impure phases have been calculated in order to determine the value of the equilibrium constant K. Ideal, ionic activities have been calculated for silicate phases such that $\alpha_{Di,Cpx} = (X_{Ca,M2})\cdot(X_{Mg,M1})$. Complete disorder on M1 and M2 is assumed for forsterite so $\alpha_{Fo,01} = (X_{Mg})^2$. Goldsmith and Newton (1969) demonstrated that calcite equilibrates with dolomite to solvus compositions in experimental runs at $T > 500°$ C. Hence, the activity for solvus equilibrated compositions is the same for experimental and natural carbonates equilibrated at the same temperature and can be neglected as the effects cancel. Energy-dispersive analysis of the carbonates in the four samples studied showed that they had no significant solid solution outside the system $CaCO_3$-$MgCO_3$. As a result, chemical analyses of carbonates in the Oaxacan assemblages would measure a change in composition due to reequilibration rather than a deviation from the experimental equilibrium composition due to solid solution. Hence, the activities of the carbonates are defined as unity for these calculations.

Using the reversals of Kase and Metz (1980), the equilibrium temperature for reaction (4) is 784° C at $P_{CO_2} = 7$ kb. The shift in the ΔG_r due to solid solution in the natural assemblage was calculated using EQUILI and is approximately 1 kj corresponding to a downward shift of 20° C. Hence, solid solutions shifts the fluid composition to $X_{CO_2} = 1$ at 764° C.

At 7 kb, reaction (4) is stable over the entire

acute angle intersection of reactions (6) and (7) is nearly $X_{CO_2} = 0.4$. The slope of reaction (5), which is tightly reversed at lower temperatures (Slaughter *et al.*, 1975; Eggert and Kerrick, 1981), becomes more horizontal over this compositional range and does not help to restrict the location of I. Calculations from Kerrick's (unpublished) 2 kb reversal of reaction (7) are inconsistent with both Kase and Metz' and Jacobs and Kerrick' reversals. For 6 kb, the calculations appear to be more consistent, however, with the location of reaction (7) required by the invariant point I than with the location required by invariant point I' (Figure 9).

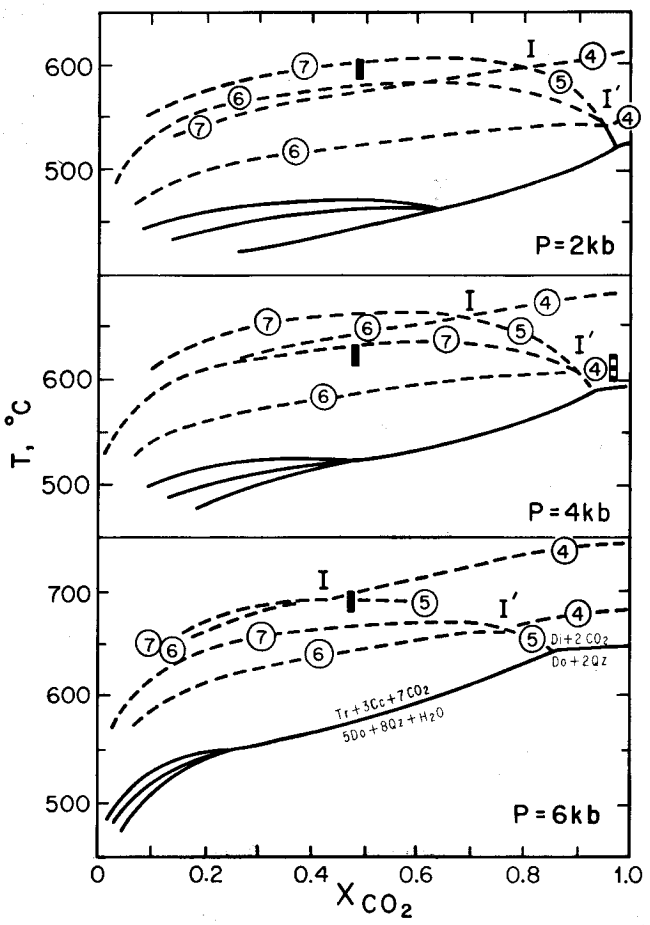

Figure 9.- $T - X_{CO_2}$ diagrams at 2, 4, and 6 kb calculated from experimental brackets for reaction (4) at 1, 3, and 5 kb (Kase and Metz, 1980) and 4 kb by Jacobs (Eggert and Kerrick, 1981), experimental data for reaction (5) at 5 kb (Slaughter *et al.*, 1975) and reaction (6) at 1, 3, and 5 kb (Metz, 1967, 1976). Other reactions are located from experimental brackets at 2, 4, and 6 kb of Eggert and Kerrick (1981). Solid rectangles have been extrapolated from a 2 kb reversal of reaction (7) (Kerrick, personal communication). I and I' are invariant points generated by the location of reaction (4) according to Kase and Metz and Jacobs reversals, respectively.

Uncertainties in experimental and thermochemical data limit the accuracy of calculation of some volatilization reactions from low pressure to higher pressures, as demonstrated by Hunt and Kerrick (1977) for the reaction rutile + calcite + quartz = sphene + CO_2. The largest differences occur when extrapolations are made over a wide range of temperature or X_{CO_2} (Jacobs and Kerrick, 1981). The inconsistency of thermochemical and experimental data may be due in part to nonideality of H_2O-CO_2 mixing and thermodynamic calculations of volatilization reactions using nonideal activities for H_2O and CO_2 calculated from the hard sphere modified Redlich-Kwong equation yields results that are in excellent agreement with the experimental data for many reactions, including reaction (4) (Jacobs and Kerrick, *op. cit.*). Figure 9 demonstrates that multiple reversals at a range of pressures for reactions (4) (Kase and Metz, 1980) and (6) (Metz, 1976) generate a self-consistent phase diagram and are thus consistent with known thermochemical data. In light of the internal consistency and consistency with other experiments and thermodynamic extrapolations from low pressures, the experimental data of Kase and Metz (1980) have been used for equilibria calculations for reaction (4).

At constant pressure and temperature, the shift in reaction equilibria due to solid solution is calculated by the equation

$$\Delta G_r(PTX\mathrm{H_2O}^2) - \Delta G_r(PTX\mathrm{H_2O}^1) = RT \ln K_{\text{solids}}$$

The activities of impure phases have been calculated in order to determine the value of the equilibrium constant K. Ideal, ionic activities have been calculated for silicate phases such that $\alpha_{\mathrm{Di,Cpx}} = (X_{\mathrm{Ca,M2}})\cdot(X_{\mathrm{Mg,M1}})$. Complete disorder on M1 and M2 is assumed for forsterite so $\alpha_{\mathrm{Fo,01}} = (X_{\mathrm{Mg}})^2$. Goldsmith and Newton (1969) demonstrated that calcite equilibrates with dolomite to solvus compositions in experimental runs at $T > 500°$ C. Hence, the activity for solvus equilibrated compositions is the same for experimental and natural carbonates equilibrated at the same temperature and can be neglected as the effects cancel. Energy-dispersive analysis of the carbonates in the four samples studied showed that they had no significant solid solution outside the system $CaCO_3$-$MgCO_3$. As a result, chemical analyses of carbonates in the Oaxacan assemblages would measure a change in composition due to reequilibration rather than a deviation from the experimental equilibrium composition due to solid solution. Hence, the activities of the carbonates are defined as unity for these calculations.

Using the reversals of Kase and Metz (1980), the equilibrium temperature for reaction (4) is 784° C at $P_{CO_2} = 7$ kb. The shift in the ΔG_r due to solid solution in the natural assemblage was calculated using EQUILI and is approximately 1 kj corresponding to a downward shift of 20° C. Hence, solid solutions shifts the fluid composition to $X_{CO_2} = 1$ at 764° C.

At 7 kb, reaction (4) is stable over the entire

range $0.2 < X_{CO_2} < 1.0$. Given the pressure estimated by garnet-orthopyroxene barometry, if the temperature can also be fixed by an independent measurement, X_{CO_2} can be estimated. The calcite-dolomite system may reequilibrate by exsolution and diffusion of Mg from calcite at lower temperature after granulite facies metamorphism (Valley and Essene, 1980b). Reequilibration of the carbonates excludes use of the calcite-dolomite solvus thermometer of Goldsmith and Newton (1969) for an internal, independent estimate of peak metamorphic temperature in the marbles. At 710° C, the temperature estimated for the complex by feldspar thermometry the assemblage dolomite + diopside + forsterite + calcite is in equilibrium for $X_{CO_2} = 0.5$. For a ±30° temperature error, the error in estimated X_{CO_2} is ±0.2.

The common presence of phlogopite-rich marbles indicates that H_2O was also a major fluid component involved in the metamorphism of these rocks. Marbles cropping out near the dolomite + diopside + forsterite + calcite assemblages contain the assemblage wollastonite + calcite + quartz, which under the same pressure-temperature conditions buffers the fluid composition to low X_{CO_2}, indicating that fluid composition varied locally at the peak of metamorphism.

CONCLUSIONS

Temperature data obtained from the Haselton and others' (1983) thermometer have been plotted on a simplified map of the study area (Figure 10). The locations of restrictive calc-silicate assemblages are also shown. Estimated pressure and temperatures (7kb, 710° C) are consistent with metamorphic conditions indicated by the occurrence of quartz + K-feldspar + garnet + sillimanite ± biotite in the pelitic gneisses and orthopyroxene + plagioclase ± garnet ± clinopyroxene in the mafic gneisses. No regional metamorphic isotherms can be delineated from the data. Little change in peak temperatures over distances of more than 50 km is typical of granulite terranes, such as the Adirondack Highlands, New York. The important role of local fluid heterogeneity has been demonstrated in the Adirondacks (Valley and Essene, 1980b; Valley and O'Neal, 1984) and deserves further study in the Oaxacan terrane.

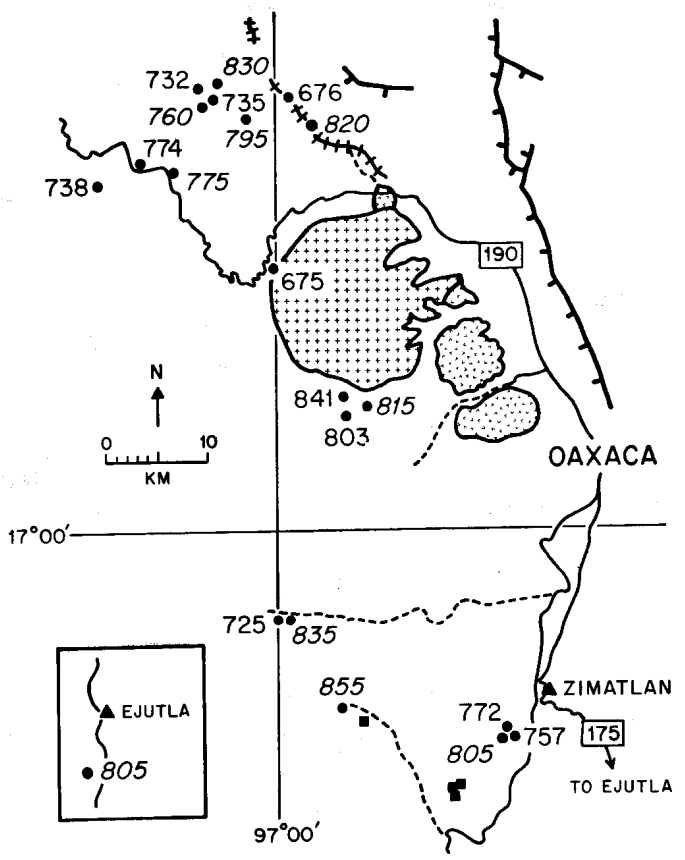

Figure 10.- Feldspar temperatures (Stormer, 1975) for the Oaxacan Complex. Temperatures suggested by the general form (Brown and Parsons, 1981) are in italics. Squares show the locations of restrictive marble assemblages for which $T = 750°$ C at $P_{CO_2} = 7$ kb. Locations are shown relative a Paleozoic granite (+) and the Oaxacan Valley anorthosite massif (v).

ACKNOWLEDGEMENTS

This research was supported by a CONOCO Fellowship (C.I.M.), Geological Society of America Penrose Grant 2885–81 (C.I.M.), and by National Science Foundation Grant EAR 81–2124 (J.W.V.). Staff members of the Dirección de Promoción Minera in Oaxaca provided logistical field support and it is published with funds of the Instituto de Geología of Universidad Nacional Autónoma de México.

REFERENCES CITED

Anderson, A. T., Jr., 1969, Massif-type anorthosite; a widespread Precambrian igneous rock: *in* Isachsen, Y. W., ed., Origin of anorthosite and related rocks. New York State Museum and Science Service, Mem. 18, p. 47–53.

Anderson, T. H., and Silver, L. T., 1971, Age of granulite metamorphism during the Oaxacan orogeny, Mexico: Geol. Soc. America, Abstr. with Programs, v. 3, p. 492 (abstract).

Birch, F., 1966, Compressibility; elastic constants: *in* Clark, S. P., Jr., ed., Handbook of physical constants. Geol. Soc. America, Mem. 97, p. 97–174.

Bloomfield, Keith, and Ortega-Gutiérrez, Fernando, 1975, Notas sobre la petrología del Complejo Oaxaqueño: Univ. Nal. Autón. México, Inst. Geología, Bol. 95, p. 23–48.

Bohlen, S. R., and Essene, E. J., 1977, Feldspar and oxide thermometry of granulites in the Adirondack Highlands: Contrib. Mineral. Petrology, v. 62, p. 153–169.

Bohlen, S. R., Essene, E. J., and Hoffman, K., 1980, Feldspar and oxide thermometry in the Adirondacks; an update: Geol. Soc. America Bull., v. 91, p. 110–113.

Bohlen, S. R., Wall, V. J., and Boettcher, A. L., 1983, Experimental investigation and application of garnet granulite equilibria: Contrib. Mineral. Petrology, v. 83, p. 52–61.

Brown, W. L., and Parsons, I., 1981, Towards a more practical two-feldspar geothermometer: Contrib. Mineral. Petrology, v 76, p. 369–377.

Buddington, A. F., and Lindsley, D. H., 1964, Iron-titanium oxide minerals and synthetic equivalents: Jour. Petrology, v. 5, pt. 2, p. 310–357.

Burnham, C. W., Holloway, J. R., and Davis, N. F., 1969, Thermodynamic properties of water to 1000° C and 10,000 bars: Geol. Soc. America, Spec. Paper 132, 96 p.

Dahl, P. S., 1979, Comparative geothermometry based on major element and oxygen isotope distributions in Precambrian metamorphic rocks from southwestern Montana: Am. Mineralogist, v. 64, p. 1280–1293.

De Waard, Dirk, 1965, The occurrence of garnet in the granulite-facies terrane of the Adirondack Highlands: Jour. Petrology, v. 6, p. 165–191.

Eggert, R. G., and Kerrick, D. M., 1981, Metamorphic equilibria in the siliceous dolomite system; 6 kbar experimental data and geologic implications: Geochim. Cosmochim. Acta, v. 45, p. 1039–1049.

Ferry, J. M., 1976, P, T, f_{CO_2}, and f_{H_2O} during metamorphism of calcareous sediments in the Waterville-Vassalboro area, south-central Maine: Contrib. Mineral. Petrology, v. 57, p. 119–143.

—1979, A map of chemical potential differences within an outcrop: Am. Mineralogist, v. 64, p. 966–985.

—1980, A case study of the amount and distribution of heat and fluid during metamorphism: Contrib. Mineral. Petrology, v. 71, p. 373–385.

—1981, Petrology of graphitic sulfide-rich schists from south-central Maine; an example of desulfidation during prograde metamorphism: Am. Mineralogist, v. 66, p. 908–930.

Fries, Carl, Jr., Schmitter-Villada, Eduardo, Damon, P. E., and Livingston, D. E., 1962, Rocas precámbricas de edad grenvilliana de la parte central de Oaxaca en el sur de México: Univ. Nal. Autón. México, Inst. Geología, Bol. 64, p. 45–53.

Fries, Carl, Jr., and Rincón-Orta, César, 1965, Nuevas aportaciones geocronológicas y técnicas empleadas en el laboratorio de geocronología: Univ. Nal. Autón. México, Inst. Geología, Bol. 73, p. 57–133.

Fries, Carl, Jr., Schlaepfer, C. J., and Rincón-Orta, César, 1966, Nuevos datos geocronológicos del Complejo Oaxaqueño: Bol. Soc. Geol. Mexicana, v. 29, p. 59–66.

Ganguly, J., and Kennedy, G. C., 1974, The energetics of natural garnet solid solutions; I, Mixing of the aluminosilicate end members: Contrib. Mineral. Petrology, v. 48, p. 137–148.

Garrison, J. R., 1979, Petrology and geochemistry of the Precambrian Coal Creek serpentinite mass and associated metamorphosed basaltic and intermediate rocks, Llano Uplift, Texas: Austin, Univ. Texas at Austin, Ph. D. dissertation, (unpublished).

—1981, Coal Creek serpentinite, Llano-Uplift, Texas; a fragment of an incomplete Precambrian ophiolite: Geology, v. 9, p. 225–230.

Gastil, R. G., and Jensky, Wallace, 1973, Evidence for strikeslip displacement beneath the Trans-Mexican Volcanic Belt: Stanford Univ. Publ. Geol. Sci., v. 13, p. 171–180.

Goldsmith, J. R., and Newton, R. C., 1969, P-T-X relations in the system $CaCO_3$-$MgCO_3$ at high temperatures and pressures: Am. Jour. Science, v. 267–A, p. 160–190.

Guidotti, C. V., Herd, H. H., and Tuttle, C. L., 1973, Composition and structural state of K-feldspars from K-feldspar + sillimanite grade rocks in northwestern Maine: Am. Mineralogist, v. 58, p. 705–716.

Harley, S. L., and Green, D. H., 1982, Garnet-orthopyroxene barometry for granulites and peridotites: Nature, v. 300, p. 697–701.

Haselton, H. T., Hovis, G. L., Hemingway, B. S., and Robie, R. A., 1983, Calorimetric investigation of the excess entropy of mixing in analbite-sanidine solid solutions; lack of evidence for Na, K short-range order and implications for two-feldspar thermometry: Am. Mineralogist, v. 68, p. 398–413.

Heath, S. A., and Fairbain, H. W., 1969, $^{87}Sr/^{86}Sr$ ratios in anorthosites and some associated rocks: *in* Isachsen, Y. W., ed., Origin of anorthosites and related rocks. New York State Museum and Science Service, Mem. 18, p. 99–110.

Hodges, K. V., and Spear, F. S., 1982, Geothermometry, geobarometry, and the triple point at Mt. Moosilauke, New Hampshire: Am. Mineralogist, v. 67, p. 1118–1134.

Holdaway, M. J., 1971, Stability of andalusite and the alumninosilicate phase diagram: Am. Jour. Science, v. 271, p. 97–131.

Hunt, J. A., and Kerrick, D. M., 1977, The stability of sphene; experimental redetermination and geologic implications: Geochim. Cosmochim. Acta, v. 41, p. 279–288.

Jacobs, G. K., and Kerrick, D. M., 1979, Experimental and thermodynamic analysis of decarbonation equilibria and the high temperature heat capacity of calcite: Trans. Am. Geophys. Union, v. 60, núm. 11, p. 406 (abstract).

—1981, Devolatilization equilibria in H_2O-CO_2 and H_2O-CO_2-NaCl fluids; an experimental and thermodynamic evaluation at elevated pressures and temperatures: Am. Mineralogist, v. 66, p. 1135–1153.

Johannes, W., 1979, Ternary feldspars; kinetics and possible equilibria at 800° C: Contrib. Mineral. Petrology, v. 68, p. 221–230.

Kase, H. R., and Metz, P., 1980, Experimental investigation of the metamorphism of siliceous dolomites; IV, Equilibrium data for the reaction: 1dolomite + 3diopside = 2forsterite + 4calcite + $2CO_2$: Contrib. Mineral. Petrology, v. 73, p. 151–159.

Matty, D. J., Leeman, W. P., and Valley, J. W., 1982, Geothermometry of crustal xenoliths from Craters of the Moon National Monument, Idaho: Geol. Soc. America, Abstr. with Programs, v. 14, p. 184 (abstract).

Mauger, R. L., and McDowell, F. W., 1982, K-Ar dating of igneous rocks in central Chihuahua, Mexico: Geol. Soc. America, Abstr. with Programs, v. 14, p. 116 (abstract).

Metz, P., 1967, Experimentelle Bildung von Forsterit und Calcit aus Tremolit und Dolomit: Geochim. Cosmochim. Acta, v. 31, p. 1517–1532.

—1976, Experimental investigation of the metamorphism of siliceous dolomites III; equilibrium data for the reaction 1tremolite + 11dolomite = 8forsterite + 13calcite + $9CO_2$+ $1H_2O$ for the total pressures of 3000 and 5000 bars: Contrib. Mineral. Petrology, v. 58, p. 137–148.

Mora, C. I., and Valley, J. W., 1985, Ternary feldspar thermometry in granulites from the Oaxacan Complex, Mexico: Contrib. Mineral. Petrology, v. 89, p. 215–225.

Nesbitt, B. E., and Essene, E. J., 1982, Metamorphic thermometry and barometry of a portion of the southern Blue Ridge Province: Am. Jour. Science, v. 282, p. 701–729.

Newton, R. C., Charlu, T. V., and Kleppa, O. J., 1980, Thermochemistry of the high structural state plagioclases: Geochim. Cosmochim. Acta, v. 41, p. 933–941.

Newton, R. C., and Haselton, H. T., 1981, Thermodynamics of the garnet-plagioclase-Al_2O_3-quartz geobarometer: *in* Newton, R. C. *et al.*, eds., Thermodynamics of minerals and melts. New York, Springer Verlag, p. 131–147.

Newton, R. C., and Perkins, D. III, 1982, Thermodynamic calibration of geobarometers based on the assemblages garnet-plagioclase-orthopyroxene (clinopyroxene)-quartz: Am. Mineralogist, v. 67, p. 203–222.

O'Hara, M. J., and Yarwood, G., 1978, High pressure-temperature point on an Archean geotherm, implied magma genesis by crustal anatexis, and consequences for garnet-pyroxene thermometry and barometry: Phil. Trans. Royal Soc. London, v. A 288, p. 441–456.

Ortega-Gutiérrez, Fernando, 1978, El Gneiss Novillo y rocas metamórficas asociadas en los cañones del Novillo y de La Peregrina, área de Ciudad Victoria, Tamaulipas: Univ. Nal. Autón. México, Inst. Geología, Revista, v. 2, p. 19–30.

—1981, Metamorphic belts of southern Mexico and their tectonic significance: Geofís. Internal. (México), v. 20, p. 177–202.

Orville, P. M., 1972, Plagioclase cation exchange equilibria with aqueous chloride solution; results at 700° and 2000 bars in the presence of quartz: Am. Jour. Science, v. 72, p. 234–272.

Padovani, E. R., and Carter, J. L., 1977, Aspects of the deep crustal evolution beneath south central New Mexico: *in* Heacock, J. C., ed., The Earth's crust. Am. Geophys. Union, Geophysics Monogr. 20, p. 14–55.

Paulson, E. G., 1964, Mineralogy and origin of the titaniferous deposit at Pluma Hidalgo, Oaxaca, Mexico: Econ. Geology, v. 59, p. 753–767.

Perkins, D. III, Essene, E. J., and Marcotty, L. A., 1982, Thermometry and barometry of some amphibolite-granulite facies rocks from the Otter Lake area, southern Quebec: Canad. Jour. Earth Science, v. 19, p. 1759–1174.

Powell, M., and Powell, R., 1977, Plagioclase-alkali-feldspar geothermometry revisited: Mineral. Mag., v. 41, p. 253–256.

Robie, R. A., Hemingway, B. S., and Fischer, J. R., 1979, Thermodynamic properties of minerals and related substances: U. S. Geol. Survey, Bull. 1452, 456 p.

Rollinson, H. R., 1979, Ilmenite-magnetite geothermometry in trondjhemites from the Scourian complex of NW Scotland: Mineral. Mag., v. 43, p. 165–170.

—1980, Iron-titanium oxides as an indicator of the role of the fluid phase during the cooling of granites metamorphosed to granulite grade: Mineral. Mag., v. 43, p. 623–631.

—1981, Garnet-pyroxene thermometry and barometry in the Scourie granulites, NW Scotland: Lithos, v. 14, p. 225–238.

—1982, Evidence from feldspar compositions of high temperatures in granite sheets in the Scourian complex, NW Scotland: Mineral. Mag., v. 46, p. 73–76.

Rucklidge, J. C., and Gasparrini, E. L., 1969, Specifications of a complete program for processing electron microprobe data; EMPADR VII: Toronto, Univ. Toronto, Dept. Geology, circular (unpublished).

Saxena, S. K., 1973, Thermodynamics of rock forming crystalling solutions: New York, Springer Verlag, 187 p.

Saxena, S. K., and Ribbe, P. H., 1972, Activity composition relations in feldspars: Contrib. Mineral. Petrology, v. 37, p. 131–138.

Seck, H. A., 1971, Der Einfluss des Drucks auf die Zusammensetzung koexistierender Alkalifeldspate und Plagioclase im System $NaAlSi_3O_8$-$KAlSi_3O_8$-$CaAl_2Si_2O_8$-H_2O: Contrib. Mineral. Petrology, v. 31, p. 67–86.

Silver, L. T., and Anderson, T. H., 1974, Possible left-lateral early to middle Mesozoic disruption of the southwestern North American craton margin: Geol. Soc. America, Abstr. with Programs, v. 6, p. 955 (abstract).

—1983, Further evidence and analysis of the role of the Mojave-Sonora megashear(s) in Mesozoic Cordilleran tectonics: Geol. Soc. America, Abstr. with Programs, v. 15, p. 273 (abstract).

Skinner, B. J., 1966, Thermal expansion: *in* Clark, S. P., Jr., ed., Handbook of physical constants. Geol. Soc. America, Mem. 97, p. 75–97.

Skippen, G. B., 1974, An experimental model for low pressure metamorphism of siliceous dolomitic marble: Am. Jour. Science, v. 274, p. 487–509.

Slaughter, J., Kerrick, D. M., and Wall, V. J., 1975, Experimental and thermodynamic study of equilibria in the system CaO-MgO-SiO_2-CO_2-H_2O: Am. Jour. Science, v. 275, p. 143–162.

Spry, A. S., 1969, Metamorphic textures: Oxford, Pergamon Press, 350 p.

Stoddard, E. F., 1980, Metamorphic conditions at the northern end of the northwest Adirondack lowlands: Geol. Soc. America Bull., v. 91, pt. II, p. 589–616.

Stormer, J. C., Jr., 1975, A practical two-feldspar thermometer: Am. Mineralogist, v. 60, p. 667–674.

Stormer, J. C., Jr., and Whitney, J. A., 1977, Two-feldspar geothermometry in granulite facies metamorphic rocks; sapphirine granulites from Brazil: Contrib. Mineral. Petrology, v. 65, p. 123–133.

Urrutia-Fucugauchi, Jaime, 1981, Paleomagnetic evidence for tectonic rotation of northern Mexico and the continuity of the Cordilleran orogenic belt between Nevada and Chihuahua: Geology, v. 9, p. 178–183.

Valley, J. W., and Essene, E. J., 1980a, Akermanite in the Cascade Slide xenolith and its significance for regional metamorphism in the Adirondacks: Contrib. Mineral. Petrology, v. 74, p. 143–152.

—1980b, Calc-silicate reactions in Adirondack marbles; the role of fluids and solid solutions: Geol. Soc. America Bull., v. 91, pt. II, p. 720–815.

Valley, J. W., and O'Neil, J. R., 1984, Fluid heterogeneity during granulite facies metamorphism in the Adirondacks; stable isotope evidence: Contrib. Mineral. Petrology, v. 85, p. 158–173.

Wall, V. J., and Essene, E. J., 1972, Subsolidus equilibrium in CaO-Al_2-O_3-SiO_2-H_2O: Geol. Soc. America, Abstr. with Programs, v. 4, p. 700 (abstract).

Whitney, J. A., and Stormer, J. C., 1977, The distribution of $NaAlSi_3O_8$ between coexisting microcline and plagioclase and its effect on geothermometric calculations: Am. Mineralogist, v. 62, p. 687–691.

Winkler, H. G. F., 1979, Petrogenesis of metamorphic rocks: New York, Springer Verlag, 348 p.

Wood, B. J., and Banno, S., 1973, Garnet-orthopyroxene and orthopyroxene-clinopyroxene relationships in simple and complex systems: Contrib. Mineral. Petrology, v. 42, p. 109–1244.